AD NUMBER: AD0469450

LIMITATION CHANGES

TO:

Approved for public release; distribution is unlimited.

FROM:

Distribution authorized to US Government Agencies only;
Export Controlled; 1 Jul 1965. Other requests shall be referred to Air Force Materials Laboratory, Wright-Patterson AFB, OH 45433.

AUTHORITY

AFSC/IST ltr dtd 21 Mar 1989

AD NUMBER

469 450

CLASSIFICATION CHANGES

TO

FROM

AUTHORITY

WR DC 1st LTR dtd 21 MAR 89
(For Entries 11 thru)

SECURITY MARKING

The classified or limited status of this report applies to each page, unless otherwise marked.
Separate page printouts MUST be marked accordingly.

THIS DOCUMENT CONTAINS INFORMATION AFFECTING THE NATIONAL DEFENSE OF THE UNITED STATES WITHIN THE MEANING OF THE ESPIONAGE LAWS, TITLE 18, U.S.C., SECTIONS 793 AND 794. THE TRANSMISSION OR THE REVELATION OF ITS CONTENTS IN ANY MANNER TO AN UNAUTHORIZED PERSON IS PROHIBITED BY LAW.

NOTICE: When government or other drawings, specifications or other data are used for any purpose other than in connection with a definitely related government procurement operation, the U. S. Government thereby incurs no responsibility, nor any obligation whatsoever; and the fact that the Government may have formulated, furnished, or in any way supplied the said drawings, specifications, or other data is not to be regarded by implication or otherwise as in any manner licensing the holder or any other person or corporation, or conveying any rights or permission to manufacture, use or sell any patented invention that may in any way be related thereto.

AFML-TR-65-2
Part I, Volume III

TERNARY PHASE EQUILIBRIA IN TRANSITION METAL-BORON-CARBON-SILICON SYSTEMS

Part I. Related Binary Systems

Volume III. Systems Mo-B and W-B

E. Rudy
St. Windisch
Aerojet-General Corporation

TECHNICAL REPORT NO. AFML-TR-65-2, Part I, Volume III
July 1965

Air Force Materials Laboratory
Research and Technology Division
Air Force Systems Command
Wright-Patterson Air Force Base, Ohio

NOTICES

When Government drawings, specifications, or other data are used for any purpose other than in connection with a definitely related Government procurement operation, the United States Government thereby incurs no responsibility nor any obligation, whatsoever, and the fact that the Government may have formulated, furnished, or in any way supplied the said drawings, specifications, or other data, is not to be regarded by implication or otherwise as in any manner licensing the holder or any other person or corporation, or conveying any rights or permission to manufacture, use, or sell any patented invention that may in any way be related thereto.

This report not releasable to (CFSTI) Clearing House for Federal Scientific and Technical Information, formerly (OTS) Office of Technical Services.

Qualified users may obtain copies of this report from the Defense Documentation Center.

The distribution of this report is limited because it contains technology identifiable with items on the Mutual Defense Assistance Control List excluded from export under U. S. Export Control Act of 1949, as implemented by AFR 400-10.

Copies of this report should not be returned to the Research and Technology Division unless return is required by security consideration, contractual obligations, or notice on a specific document.

AFML-TR-65-2
Part I, Volume III

TERNARY PHASE EQUILIBRIA IN TRANSITION METAL-BORON-CARBON-SILICON SYSTEMS

Part I. Related Binary Systems

Volume III. Systems Mo-B and W-B

E. Rudy
St. Windisch
Aerojet-General Corporation

FOREWORD

The work described in this report was performed at the Materials Research Laboratory, Aerojet-General Corporation, Sacramento, California, under USAF Contract No. AF 33(615)-1249. The contract was initiated under Project No. 7350, Task No. 735001. The work was administered under the direction of the Air Force Materials Laboratory, Research and Technology Division, with Captain R.A. Peterson acting as Project Engineer, and Dr. E. Rudy, Aerojet-General Corporation, as Principal Investigator. Professor Dr. Hans Nowotny, University of Vienna, served as consultant to the project.

The project, which includes the experimental and theoretical investigation of selected ternary systems in the system classes Me_1-Me_2-C, Me-B-C, Me_1-Me_2-B, Me-Si-B, and Me-Si-C, was initiated on 1 January 1964.

The phase diagram work was performed by E. Rudy and St. Windisch. Assisting in the experimental investigations were: J. Pomodoro (preparation of sample material), D. P. Harmon and T. Eckert (DTA-runs), J. Hoffman (metallographic preparations), and R. Cobb (X-ray exposures). The help of Dr. A. J. Stosick in mounting a large portion of the numerous samples for the metallographic examinations is gratefully acknowledged.

Chemical analysis of the alloys was performed under the supervision of Mr. W. E. Trahan, Quality Control Division of Aerojet-General Corporation. The authors also wish to thank Mr. R. Cristoni who prepared the illustrations and Mrs. J. Weidner, who typed the report.

ABSTRACT

On the basis of X-ray, melting point, metallographic, and differential thermoanalytical studies on molybdenum-boron and tungsten-boron alloys, constitution diagrams for both binary systems are presented. In the high temperature regions, the newly established phase diagrams differ significantly from previously reported systems.

The results are discussed and compared with available literature data.

TABLE OF CONTENTS

ILLUSTRATIONS

ILLUSTRATIONS (Cont'd)

ILLUSTRATIONS (Cont'd)

ILLUSTRATIONS (Cont'd)

TABLES

I. INTRODUCTION AND SUMMARY

A. INTRODUCTION

Borides and boride-containing alloys have found commercial application as base materials for oxidation- and wear-resistant parts. Their corrosion resistance towards specific chemical agents has stimulated their use in hot-gas valves, corrosion resistant claddings, tubings, fittings, etc.

Like other interstitial type compounds such as the carbides, nitrides, and, to a certain degree, the silicides of the refractory transition metals, the borides are extremely brittle and hence sensitive to mechanical or thermal shock loads. The concept of boride-metal composites, which would eliminate certain difficulties arising from the brittleness of these compounds, is not new, and has been followed for quite some time[1]; very little systematic work, however, has been done on the study of the phase interactions in systems with more than two components. To a part, this scarcity of data has to be attributed to the complexity of the phase relations as well as to the experimental difficulties(extremely slow attainment of equilibrium, container problems, etc.) encountered in the investigation of the phase relationships in this system class.

The major task in the investigations of boride systems performed under this program concerns the investigation of ternary systems Me_1-Me_2-B, where Me_1 and Me_2 stands for a refractory transition metal. During the course of the work on the ternaries,certain inconsistencies of our data with the previously reported binary systems became apparent; the investigation of selected binary metal-boron systems was therefore initiated as a subtask to the investigation of the ternary phase diagrams.

The present report, which is the first in the series of reports on binary metal-boron systems, contains the work performed on the systems molybdenum-boron and tungsten-boron.

Other binary systems which have been investigated include Ti-B, Zr-B, Hf-B, Nb-B, and Ta-B. The work on these systems will be described in two follow-on reports.

B. SUMMARY

Using hot-pressed, sintered and quenched, as well as arc-melted alloys, the binary systems molybdenum-boron and tungsten-boron were investigated by X-ray, metallographic, DTA, and melting point techniques. Phase diagrams for both systems were established (Figures 1 and 2).

1. Molybdenum-Boron (Figure 1, Table 1)

With the exception of Mo_3B_2, all previously reported intermediate phases were confirmed in this investigation. In the high temperature region, the newly established data differ significantly from previous investigations.

a. The Molybdenum Phase

The melting point of molybdenum was determined to 2619°. The solid solubility limit of boron in molybdenum at the Mo-Mo_2B eutectic temperature (2175°C) is below 2 atomic percent.

b. Mo_2B

Mo_2B, with a tetragonal, C16-type of crystal structure (a = 5.547 Å, c = 4.742 Å), decomposes in a peritectic reaction at 2280°C into β-MoB and melt. The phase is confined to compositions close to the stoichiometric.

A eutectic is formed between Mo and Mo_2B. The eutectic point is located at 23 At% B and a temperature of 2175°C.

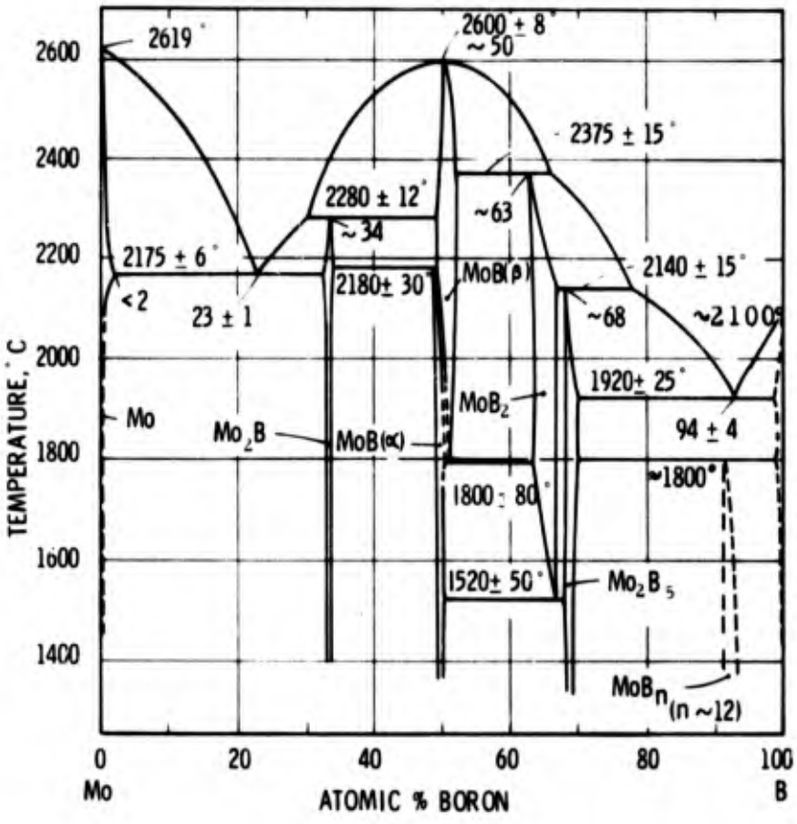

Figure 1. Constitution Diagram Molybdenum-Boron

(The Temperature Figures Given Refer to the Precision of the Measurements and do not Include Errors in the Pyrometer Calibration)

c. The Monoboride Phases

Two phases exist at boron concentrations around 50 At%:

α-MoB, with a tetragonal Bg-type of structure, extends from 48 to ~50 At% B at 1800°C (a = 3.103 Å, c = 16.97 Å, to

Table 1. Isothermal Reactions in the System Molybdenum-Boron

Temperature, °C	Reaction	Composition of the Equilibrium Phases, At% B			Type of Reaction
2619°	$L \leftrightarrow Mo$	0	0	0	Melting Point of Molybdenum
2600°	$L \leftrightarrow \beta\text{-MoB}$	~50	~50	-	Congruent Transformation
2375°	$L + \beta\text{-MoB} \leftrightarrow MoB_2$	~66	52	~63	Peritectic Reaction
2280°	$L + \beta\text{-MoB} \leftrightarrow Mo_2B$	~30	49	34	Peritectic Reaction
2180°	$Mo_2B + \beta\text{-MoB} \leftrightarrow \alpha\text{-MoB}$	34	~49	~48.5	Peritectoid Reaction
2175°	$L \leftrightarrow Mo + Mo_2B$	23	< 2	33	Eutectic Reaction
2140°	$L + MoB_2 \leftrightarrow Mo_2B_5$	~78	66	68	Peritectic Reaction
≈2100°	$L \leftrightarrow B$	100	100	-	Melting Point of Boron
1920°	$L \leftrightarrow Mo_2B_5 + B$	~94	70	~98	Eutectic Reaction
1800°	$\beta\text{-MoB} \leftrightarrow \alpha\text{-MoB} + MoB_2$	~51	~50.5	63	Eutectoid Reaction
≈1800°	$Mo_2B_5 + B \leftrightarrow MoB_{\sim 12}$	70	~99	~90	Peritectoid Reaction
1520°	$MoB_2 \leftrightarrow \alpha\text{-MoB} + Mo_2B_5$	66	50	67	Eutectoid Reaction

a = 3.114 Å, c = 16.95 Å). The phase is stable from room temperature up to 2180°C, where it decomposes in a peritectoid reaction into Mo_2B and β-MoB.

β-MoB, with an orthorhombic CrB-type of structure, extends from 48 to 51 At% boron at 2200°C (a = 3.145 Å, b = 8.472 Å, c = 3.063 Å, to a = 3.150 Å, b = 8.488 Å; c = 3.082 Å). The phase melts congruently at 2600°C at a composition of ~50 At% B, and decomposes in a slow eutectoid reaction at approximately 1800°C into α-MoB and MoB_2.

d. MoB_2

MoB_2, with a simple hexagonal, C32 type of structure, is confined to the compositional limits 63 to 66 At% B, (a = 3.044 Å, c = 3.062 Å, to a = 3.041 Å, c = 3.072 Å). The phase, which melts incongruently at 63 At% B and 2375°C, decomposes in a slow eutectoid reaction at approximately 1520°C into α-MoB and Mo_2B_5

e. Mo_2B_5

Mo_2B_5, with a rhombohedral $D8_i$-type of structure [a = 3.005 Å, c = 21.00 Å, to a = 3.012 Å, c = 20.92 Å, (hexagonal axes)] and a narrow range of homogeneity (68-69 At% B), decomposes in a peritectic reaction at 2140°C into the diboride and melt. A eutectic is formed between Mo_2B_5 and boron (94 ± 4 At% B, 1920°C).

f. $MoB_{\sim 12}$

The structure of this high-boron (~ 90 At% B) phase has not yet been clarified. The diffraction pattern shows similarity to the MoB_2 as well as the Mo_2B_5-type. This relationship is also expressed by the fact that the strongest diffraction lines can be

indexed on the basis of a simple hexagonal subcell with a = 3.004 Å, c = 3.175 Å. The experiments indicate that the phase decomposes above ~1800°C.

2. Tungsten-Boron (Figure 2 and Table 2)

The phases W_2B, α- and β-WB, W_2B_5, and $WB_{\sim 12}$, all of which had been described earlier in the literature, were confirmed in this investigation. The previously reported phase diagram was based on estimates only.

a. The Tungsten Phase

For pure tungsten, a melting point of 3423 ± 20°C was determined. The solid solubility of boron in tungsten is below 1 atomic percent at the W-W_2B eutectic temperature (2600°C).

b. W_2B

Ditungsten boride, with a tetragonal, C16-type of crystal structure (a = 5.570 Å, c = 4.744 Å to a = 5.572 Å, c = 4.746 Å), melts congruently at 2670°C. The width of the homogeneous range is below 2 atomic % boron over the entire solidus range. Between tungsten and W_2B a eutectic is formed at 27 At% B and 2600°C.

c. The Monoboride Phases

Two intermediate phases are formed in the equiatomic concentration region.

α-WB, with a tetragonal, B_g-type of structure, extends from 48 to approximately 51 atomic % boron at 2100°C (a = 3.093 Å, c = 16.99 Å, to a = 3.120 Å, c = 16.99 Å). The phase is stable from room temperature up to ~2170°C, where it decomposes in a peritectoid reaction into β-WB and W_2B_5.

β-WB with an orthorhombic, CrB-type of structure (a = 3.142; b = 8.506, c = 3.065 Å in excess W_2B containing alloys) extends from approximately 48 to 52 atomic percent boron (2200 to 2400°C) and melts congruently at 2665° at a composition of ~48 At% B.

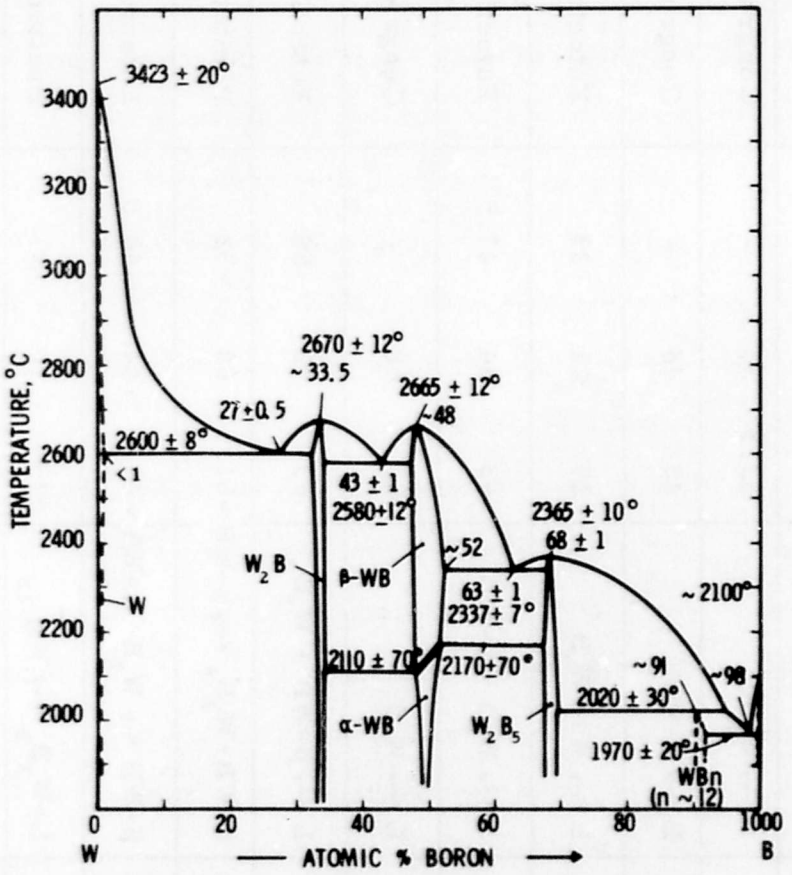

Figure 2. Constitution Diagram Tungsten-Boron

(The Temperature Figures Refer to the Precision of the Measurements and do not Include Errors in the Pyrometer Calibration)

It forms eutectic equilibria with W_2B (43 At% B, 2580°C) and W_2B_5 (63 At% B, 2337°C), and decomposes in a rapid eutectoid reaction at ~2110°C into W_2B and α-WB.

Table 2. Isothermal Reactions in the System Tungsten-Boron

Temperature, °C	Reaction	Composition of the Equilibrium Phases, At% B			Type of Reaction
3423°	$L \leftrightarrow W$	0	0	0	Melting Point of Tungsten
2670°	$L \leftrightarrow W_2B$	33.5	33.5	-	Congruent Transformation
2665°	$L \leftrightarrow \beta$-WB	48	48	-	Congruent Transformation
2600	$L \leftrightarrow W + W_2B$	27	<1	33	Eutectic Reaction
2580°	$L \leftrightarrow W_2B + \beta$-WB	43	34	47.5	Eutectic Reaction
2365°	$L \leftrightarrow W_2B_5$	68	68	-	Congruent Transformation
2337°	$L \leftrightarrow \beta$-WB + W_2B_5	63	52	68	Eutectic Reaction
2170°	β-WB+$W_2B_5 \leftrightarrow \alpha$-WB	~51.5	68	~52	Peritectoid Reaction
2110°	β-WB $\leftrightarrow W_2B + \alpha$-WB	~48	~44	~48.5	Eutectoid Reaction
2020°	$L+W_2B_5 \leftrightarrow WB_{\sim 12}$	~95	70	~91	Peritectic Reaction
1970°	$L \leftrightarrow WB_{\sim 12} + B$	~98	~91	>99	Eutectic Reaction

d. W_2B_5

W_2B_5, with a hexagonal, $D8_h$-type of structure, melts congruently at 2365°C at a composition of 68 At% B. Its concentration range of existence is confined to the limits 67 to 70 At% B (a = 2.980 Å, c = 13.88 Å, to a = 2.986 Å, c = 13.90 Å).

e. $WB_{\sim 12}$

Tungsten dodecaboride of unknown crystal structure, but isomorphous with $MoB_{\sim 12}$, melts congruently at approximately 2020°C. It forms a eutectic with boron (~98 At% B, 1970°C).

II. LITERATURE REVIEW

A. MOLYBDENUM BORON

The existence of at least six intermediate phases, Mo_2B, α- and β-MoB, MoB_2, Mo_2B_5, and $MoB_{\sim 12}$ has been ascertained from previous investigations (Table 3). The clarification of the crystal structures of the phases in the Mo-B system is mainly due to R. Kiessling[2] and R. Steinitz and co-workers[3]. The currently accepted phase diagram, based mainly on the investigations by R. Steinitz, et.al.[3], and P. W. Gilles and B.D. Pollock[4], is shown in Figure 3.

Mo_2B and MoB were prepared by G. Weiss and L. Andrieux[5] by electrolytic deposition from salt-melts. According to R. Kiessling[2] Mo_2B is formed stoichiometrically and has a tetragonal ($CuAl_2$-type) crystal structure (Table 3). The low temperature modification of MoB is body centered tetragonal[2] (Bg-type). β-MoB, stable only at temperatures above 2000°C[3], has an orthorhombic CrB-type of structure.

Mo_2B_5 (rhombohedral [2, 6], Table 3), occurs at slightly under-stoichiometric compositions (~ 70 At%[2]). R. Steinitz, et.al.[3] give the homogeneity limits to 68.2 and 70 At% B. MoB_2 (hexagonal C32-type) first prepared electrolytically by Bertaut and Blum[7] was later reported as a high temperature phase, stable only between 1600° and 2100°C[3].

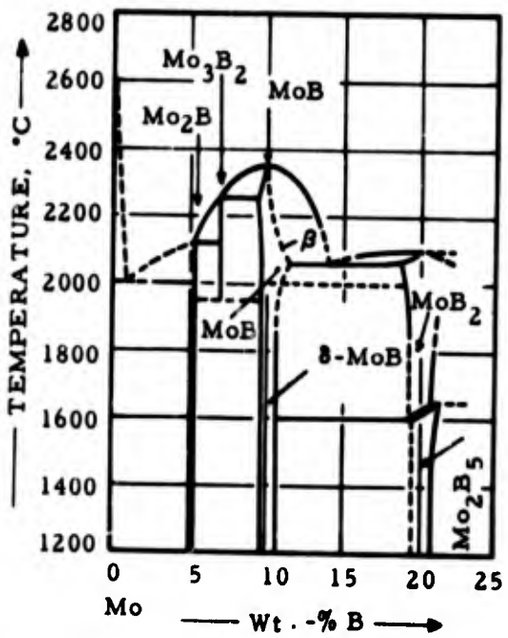

Figure 3. Phase Diagram Molybdenum-Boron
(After R. Kieffer and F. Benesovsky, 1963)

The Diagram is Based on Work by R. Steinitz, I. Binder, and D. Moskowitz (1952), and by P. W. Gilles and B. D. Pollock (1953).

A. Chretien and J. Helgorsky[8] ascribe a tetragonal structure to a compound MoB_4. The occurrence of a boron-rich phase $MoB_{\sim 12}$ was also noted in investigations by E. Rudy, et.al.[9]. A comparison of the diffraction patterns showed this phase to be identical with the previously

Table 3. Structure and Lattice Parameters of Molybdenum Borides

Phase	Structure	LATTICE PARAMETERS, ÅNGSTROM Literature	This Investigation
Mo_2B	Tetr, C16, $CuAl_2$-Type	a = 5.543 c = 4.735 (2) a = 5.547 c = 4.740 (3)	Mo+Mo_2B a = 5.547 c = 4.742 Mo_2B+MoB a = 5.547 c = 4.740
MoB Low Temp. modif.	Tetr., Bg	a = 3.105 c = 16.97 at 48.8 At%B a = 3.110 c = 16.95 at 50 At%B (2) a = 3.11 c = 16.97 (6) (3) a = 3.103 c = 16.95 (9)	Mo_2B+MoB a = 3.103 c = 16.97 MoB+MoB_2 a = 3.114 c = 16.95
β-MoB High Temp. modif.	Orthorhomb. B_f CrB-Type	a = 3.166 b = 8.61 c = 3.08 (3) a = 3.151 b = 8.47$_0$ c = 3.082 (9)	Mo_2B+MoB a = 3.145 b = 8.472 c = 3.063 51 At% B a = 3.150 b = 8.488 c = 3.082
MoB_2	hex., C32-AlB_2-Type	a = 3.05 c = 3.113 (7) a = 3.06 c = 3.10 (3) a = 3.039 to 3.027 c = 3.055 to 3.120 (9) (Arcmolten alloys)	MoB+MoB_2 a = 3.044 c = 3.062 MoB_2+Mo_2B_5 a = 3.041 c = 3.072
Mo_2B_5	rhombohedral $D8_i$	a = 3.011 c = 20.93 (2) a = 3.01 c = 20.93 (3) a = 3.009 c = 20.92 (9) (hexagonal axes)	MoB_2+Mo_2B_5 a = 3.005 c = 21.00 Mo_2B_5+$MoB_{\sim 12}$ a = 3.012 c = 20.92
Mo_3B_2	tetragonal U_3Si_2-Type	(3) a = 6.002 c = 3.146 (10)	not observed
MoB_4 $MoB_{\sim 12}$	tetragonal n.d.	a = 6.34 c = 4.50 (8) a = 3.004 c = 3.174 (9) Simple hexagonal Subcell	n.d. a = 3.004 c = 3.175 } hexagonal subcell

described MoB_4. The structure of this phase which shows similarity to the C32-type as well as the related structure of Mo_2B_5, is unknown. A simple hexagonal subcell a = 3.004 Å, c = 3.174 Å was derived by E. Rudy, et.al.[9]. These subcell dimensions relate to the tetragonal axes proposed by Chretien and J. Helgorsky by $a = 2c_{subcell}$, and $c = a_{subcell}\sqrt{2}$.

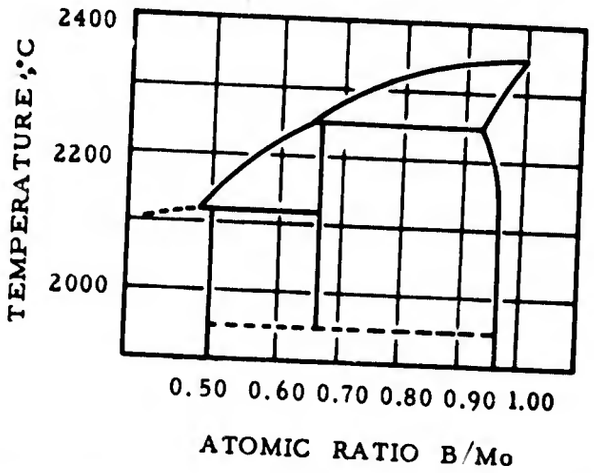

Figure 4. Partial Phase Diagram Molybdenum-Boron
(P.W. Gilles and B. D. Pollock, 1953)

The existence of a high temperature phase Mo_3B_2 was claimed by R. Steinitz, et.al.[3] and was said to be isomorphous with Cr_3B_2 (Cr_5B_3). The occurrence of (apparently) the same compound at compositions of 40 At% B was also noted in the experiments by P. W. Gilles and B.D.Pollock. A. Wittman, H. Nowotny, and H. Boller[10] suggest a U_3Si_2-type of structure (a = 5.99 Å, c = 3.14 Å). The existence of this compound was doubted by E. Rudy, et.al.[9], who attributes previous findings to carbon-contamination of the alloys.

On the basis of X-ray and melting point studies, a phase diagram of the system was proposed by R. Steinitz, et.al.[3]. Somewhat higher melting temperatures for the intermediate phases were found by

P. W. Gilles and B. D. Pollock[4] in a subsequent partial reinvestigation of the system (Table 4 and Figure 4). The solid solubility of boron in molybdenum is very low[11].

B. TUNGSTEN-BORON

R. Kiessling[2], investigating the system at temperatures below 1200°C, reports three intermediate phases (Table 5).

W_2B, isomorphous with Mo_2B (tetrag.$CuAl_2$-type) has a very small homogeneity range; WB, with a tetragonal (Bg-type) crystal structure, extends from 48 to 50.5 At% B. W_2B_5 (hexagonal, $D8_h$-type), extends from 66.7 - 68 At% B. In later investigations, B. Post and F.W. Glaser[13] found at compositions around 50 At% B a high temperature phase (β-WB), which is stable only at temperatures above 1850°C. β-WB has an orthorhombic, CrB-type of structure and is isomorphous with the high temperature phase in the Mo-B system. In sintered high boron alloys, A. Chretien and J. Helgorsky,[8] observed the formation of a new compound WB_4 and indexed the diffraction pattern on the basis of a tetragonal unit cell. Apparently the same compound was prepared in the investigations by E. Rudy, et.al.[9] and,according to the composition where it was found in pure form, was designated as $WB_{\sim 12}$. The structure of this phase, which is isomorphous with the analogous compound in the Mo-B system, is still unknown. Similarity to the C32-type as well as the Me_2B_5 types is expressed in the fact, that the strongest diffraction lines can be indexed on the basis of a simple hexagonal subcell with a = 3.994 Å, and c = 3.174 Å[9].

Samsonov[14] reported the homogeneity limits for WB to lie between 44.4 and 55 At% B, and for W_2B_5 between 68 and 75 At% B.

Table 4. Melting Temperatures of Molybdenum-Boron Alloys (Literature Values)

	Temperature, °C	Composition, At% B	Investigator	Ref
Mo-Mo_2B Eutectic	2000°	~8	Steinitz, Binder, and Moskowitz, 1952	3
	<2100°		Gilles and Pollock, 1953	4
	2180°	20(estim.)	Climax Molybdenum Company	11
Mo_2B (peritectic decomposition)	2000°	~33.3	Steinitz, Binder, and Moskowitz, 1952	3
	<2142°	~33.3	Gilles and Pollock, 1953	4
Mo_3B_2 (peritectic decomposition)	2070°	~40	Steinitz, Binder, and Moskowitz, 1952	3
	2221 - 2266°	~40	Gilles and Pollock, 1953	4
MoB	2180°	~50	Steinitz, Binder, and Moskowitiz, 1952	3
	2325 - 2374°	~50	Gilles and Pollock, 1953	4
MoB-MoB_2 Eutectic	2060°	~59	Steinitz, Binder, and Moskowitiz, 1952	3
MoB_2	2100°	~70	Steinitz, Binder, and Moskowitz, 1952	3
	2250°		Kieffer, Benesovsky, and Honak, 1952	12

Table 5. Structure and Lattice Parameters of Tungsten Borides

Phase	Structure	LATTICE PARAMETERS, ÅNGSTRÖM	
		Literature Values	This Investigation
W_2B	Tetr., C16-$CuAl_2$-Type	a = 5.564 c = 4.740 (2) a = 5.566 c = 4.748	W+W_2B: a = 5.570 c = 4.744 W_2B+WB: a = 5.572 c = 4.746
WB Low Temp. Modif.	Tetrag., Bg-Type	a = 3.115 c = 16.93 (2) a = 3.110 c = 16.95 (9)	W_2B+WB: a = 3.093 c = 16.99 WB+W_2B_5: a = 3.120 c = 16.99
β- WB High Temp Modif.	Orthorhomb. CrB-Type	a = 3.19 b = 8.40 (13,15) c = 3.07	W_2B+WB: a = 3.142 b = 8.506 c = 3.065
ε-W_2B_5	hex., $D8_h$-Type	a = 2.982 c = 13.87 (2) WB+W_2B_5: a = 2.984 c = 13.87 (9) W_2B_5+$WB_{\sim 12}$: a = 2.984 c = 13.89	WB+W_2B_5: a = 2.980 c = 13.88 W_2B_5+$WB_{\sim 12}$: a = 2.986 c = 13.90
WB_4 $WB_{\sim 12}$	Tetr.	a = 6.34 c = 4.50 (8) a = 3.994 c = 3.174 (9) (Simple Hexagonal Subcell)	n.d. a = 3.994 c = 3.174 (hex. subcell)

Melting point data on tungsten borides are very scarce and are, to a large part, estimates (Table 6). On the basis of the available literature information, a tentative phase diagram of the system was proposed by R. Kieffer and F. Benesovsky[1] and is shown in Figure 5.

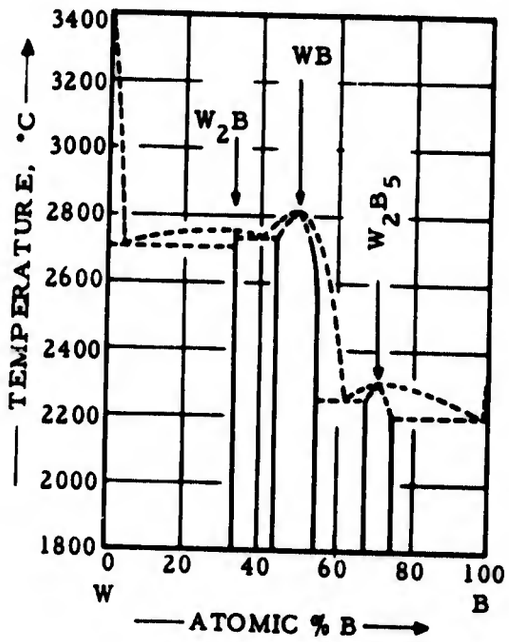

Figure 5. Tentative Phase Diagram Tungsten-Boron
(After R. Kieffer and F. Benesovsky, 1963)

Table 6. Melting Temperatures of Tungsten-Boron Alloys (Literature Values)

	Temperature, °C	Composition, At% B	Investigator	Ref
W-W_2B Eutectic	Above 2000°		Brewer, et.al., 1951	16
	2700° (Estimated)	~4	Kieffer and Benesovsky, 1963	1
W_2B	2700°		Honak, 1951	17
	Above 2000°		Brewer, et.al., 1951	16
W_2B-WB Eutectic	2730° (Estimated)	~41	Kieffer and Benesovsky, 1963	1
WB	2920°	~50 (?)	Agte, 1931	18
	2860°		Honak, 1951	17
WB-W_2B_5 Eutectic	2250° (Estimated)	~62	Kieffer and Benesovsky, 1963	1
W_2B_5	~ 2300°		Schwarzkopf and Glaser, 1953	19
	Above 2000°		Brewer, et.al., 1951	16

III. EXPERIMENTAL PROGRAM

A. EXPERIMENTAL PROCEDURES

1. Starting Materials

The elemental powders as well as MoB_2 and W_2B_5 served as starting materials for the preparation of the experimental alloy material.

The molybdenum powder (Wah Chang Corporation, Albany, Oregon) had the following impurities (contents in ppm): Al-100, C-136, Co-50, Cr-< 50, Cu-< 100, Fe-< 20, Ni-40, O-1120, Pb-< 100, Si-< 200, Ti-< 50, N-100. No second phase impurity could be found in strongly overexposed powder patterns, and a lattice parameter of $a = 3.147_3$ Å was obtained from an exposure with CuK_α radiation.

Boron powder with a purity of 99.55% was purchased from United Mineral and Chemical Corporation, New York. Major impurities were iron (0.25%) and carbon(0.1%).

MoB_2 was prepared by direct reaction of the elements. The well-blended mixture of the molybdenum and boron-powder was cold-compacted under a pressure of 4 tons per cm^2, and loaded inside a tantalum can into a carbon-pot furnace. The reaction, which initiated at about 1200°C, was completed by a 2 hour vacuum treatment at 1750°C. The resulting reaction cake was then comminuted in hard metal lined ball mills to a grain size < 44 micrometers and the cobalt traces, picked up during milling, were removed by an acid-leach in 6N hydrochloric acid. The following impurities were found spectrographically (ppm): Fe-500, Si-200, Mg-100, Al-500, Ca-400, Co-< 100, Cu-< 100, Ni-< 100, Mn-< 100, Cr-< 100, Ti-50.

The elements, V, W, Ta, and Nb were present in undetectable amounts only. The product which also contained 0.116 Wt% carbon, had a total boron content of 66.0 $\pm$ 0.5 At%. X-ray analysis showed the diboride (a = 3.041 Å, c = 3.072 Å) accompanied by minute traces of Mo_2B_5.

For the investigations in the tungsten-boron system, tungsten, boron and W_2B_5 were used for the alloy preparation.

The tungsten powder (Wah Chang Corporation, Albany, Oregon) had the following impurities (in ppm): Mo-50, O-720, Fe-40, Ni-20, sum of all other impurities -< 60. The lattice parameter, calculated from an X-ray exposure with CuK_α-radiation was a = 3.166$_5$ Å.

Preparation and processing of W_2B_5 was identical with the procedures described for MoB_2. The total boron content of the boride was 70.7 $\pm$ 0.5 At% B; it also contained initially 0.6 Wt% carbon, which, after reheating with the corresponding amount of tungsten oxide, was reduced to 0.12 Wt%.

The following impurities were determined spectrographically (in ppm): Fe-550, Si-100, Mg-100, Al-500, Ca-100, Cu-100, Ni-100, Mn-100, Cr-100, Mo-100, Ti-600. From an exposure with CuK_α-radiation, lattice parameters of a = 2.982 Å, and c = 13.88 Å were calculated.

2. Sample Preparation

Short duration hot-pressing[20] (1500 - 2000°C) of the well blended powder mixtures was exclusively used for the preparation of the experimental alloy material. Melting point and DTA-specimens were used in the as-hot pressed condition. The heat-treatment schedules for the alloys prepared for the investigation of the solid state reactions are listed in Table 7.

Quenching of the alloys was achieved by dropping the specimen — after equilibration at the desired temperature — into a preheated (~ 300°C) tin bath. Studies of the reaction kinetics at intermediate cooling rates (0.2 to 80°C per second) were carried out in the DTA as well as in the Pirani-apparatus[20].

Table 7. Heat Treatment of Molybdenum-Boron and Tungsten-Boron Alloys

Alloys	Equilibration Treatment		
	Temperature	Duration (Hours)	Atmosphere
Mo-B	1400°C	140	Vac., 2.10^{-5} Torr
	1700°C	72	Vac., 2.10^{-5} Torr
	1800°C	11	High Purity Helium
W-B	2100°C	4	Helium
	2000°C	8	Helium
	1700°C	72	Vac., 2.10^{-5} Torr

3. Melting Temperatures and Differential-Thermoanalytical Studies

The melting temperatures of the alloys were determined with the Pirani-technique and were carried out under high purity helium (~ 1 atm). Equipment and calibration procedures have been described previously[20]. The DTA-runs were performed under ambient helium pressure as well as under vacuum. The results were identical.

4. Metallography

The specimens were mounted in an (electrically) conductive mixture of diallylphtalate-lucite-copper powder. After coarse grinding on silicon carbide powder (grit sizes varying between 120 and 600),

the samples were polished on Microcloth, using a suspension of 0.05 micron alumina in a solution of 1 part Murakamis reagent in 99 parts of water. Molybdenum-boron alloys were etched electrolytically in a 10% aqueous oxalic acid solution. Tungsten-boron alloys were electroetched in 2% NaOH. No etching was required for alloys with boron contents above 70 atomic percent.

5. X-Ray Analysis

X-ray powder patterns with Cu-K_α-radiation were prepared from all alloys prepared in the course of the investigations. The films were measured on a Siemens-Kirem coincidence scale.

6. Chemical Analysis*

Dissolution of the powdered borides was achieved by fusion in pre-dried sodium carbonate at 1000°C. The resulting melt was dissolved in water, and excess carbonate removed by barium hydroxide. After removal of the precipitates, boric acid was determined by differential titration of the boro-mannitol complex with N/10 NaOH between p_H-values of 5.3 and 8.5. Depending on the sample material, the consistency of data obtained by this method varied between $\pm$ 0.1 and $\pm$ 1 At% B absolute.

Carbon analysis was performed using the standard combustion technique. Oxygen, nitrogen and hydrogen were determined by the gas fusion technique, and small impurity contents were determined in a semiquantitative way spectrographically.

---

*The chemical analysis were performed under the supervision of Mr. W. E. Trahan, Metals and Plastics Chemical Testing Laboratory of Aerojet-General Corporation.

B. RESULTS

1. Molybdenum-Boron

a. The Concentration Range Mo-Mo_2B

A total of approximately 80 alloys were prepared in this alloy system.

Starting with pure molybdenum, the incipient temperatures drop rapidly from 2619°C, the melting point of molybdenum, to 2175°C, the eutectic reaction isotherm Mo-Mo_2B, (Table 8). While alloy compositions up to total boron concentrations showed typical two-phase (heterogeneous) melting, the alloy compositions 20 and 25 At% B melted practically isothermal. Two-phase melting was again noticed at boron concentrations above 30 At%.

The observed melting pattern indicates the eutectic composition to lie in the vicinity of 25 atomic % boron. This was subsequently confirmed by metallographic inspection of melted and quenched alloys (Figures 6 to 12). The precipitation of boride within the molybdenum grains (Figure 6) indicate a slight boron solubility (< 2 At%) at high temperatures (> 2000°C). While the alloy with 20 At% B still shows smaller quantities of primary crystallized molybdenum (Figure 9), the specimen with 25 At% B (Figure 12) is already slightly hypereutectic. The eutectic concentration was finally bracketed by an alloy with 23 At% B, which, after quenching from the molten state, exhibited a pure eutectic structure (Figure 13).

Table 8. Melting Temperatures of Molybdenum-Boron Alloys and Qualitative Phase Evaluation After Melting

No.	At% B Nom.	At% B Anal.	Melting Temp. °C Incipient	Melting Temp. °C Collapse	Melting	Phases Present After Melting (X-Ray, Molten Portion)	Metallography
1	0	0	2619		Sharp	(pure Mo)	n. d.
2	2	n. d.	2259	2593	Heterogeneous	n.d.	Two-Phase
3	5	n. d.	2207	2485	Heterogeneous	n.d.	Mo + Eutectic
4	10	9.7	2161	2240	Heterogeneous	Mo + Mo_2B	Mo + Eutectic
5	15	n. d.	2176	2185	Heterogeneous	Mo + Mo_2B	Mo + Eutectic
6	20	n. d.	2176	2176	Fairly Sharp	Mo + Mo_2B	Mo + Eutectic
7	25	n. d.	2176	2176	Sharp	Mo + Mo_2B	Mo_2B + Eutectic
8	30	n. d.	2181	2186	Slightly Heterog	Mo + Mo_2B	Mo_2B + Metal
9	33	33.4	2176	2274	Heterogeneous	Mo_2B + Trace Mo	Mo_2B
10	35	33.8	2276	2290	Heterogeneous	Mo_2B + Trace α-MoB	Mo_2B + Traces MoB
11	38	n. d.	2279	2295	Heterogeneous	Mo_2B + α-MoB + β-MoB	n. d.
12	40	n. d.	2285	2300	Heterogeneous	Mo_2B + β-MoB	Mo_2B + MoB(+ Me)
13	43	n. d.	2296	2480	Heterogeneous	Mo_2B + β-MoB	n. d.
14	45	n. d.	2325	2586	Heterogeneous	Mo_2B + α-MoB + β-MoB	Mo_2B + MoB
15	48	48.2	2336	2600	Sharp Collapse	Mo_2B(Trace) + α-MoB + β-MoB	MoB
16	50	n. d.	2600	2600	Sharp	α-MoB + β-MoB + Trace Mo_2B	MoB
17	51	50.6	2590	2595	Slightly Heterog	β-MoB	MoB
18	52	n. d.	2430	2542	Heterogeneous	β-MoB	MoB
19	54	n. d.	2399	2466	Heterogeneous	β-MoB + -MoB_2	MoB + MoB_2
20	56	n. d.	2390	2416	Heterogeneous	β-MoB + Trace α-MoB + MoB_2	MoB_2 + MoB
21	59	n. d.	2390	2403	Slightly Heterog	β-MoB + MoB_2	n. d.
22	62	n. d.	2377	2377	Fairly Sharp	Trace β-MoB + MoB_2	MoB_2
23	64	63.8	2356	2377	Heterogeneous	MoB_2	MoB_2
24	65	n. d.	2330	2372	Heterogeneous	MoB_2 + Trace Mo_2B_5	n. d.
25	66	n. d.	2264	2341	Heterogeneous	MoB_2 + Trace Mo_2B_5	n. d.
26	67	67.2	2155	2310	Heterogeneous	MoB_2 + Mo_2B_5	n. d.
27	68	68.2	2148	2240	Heterogeneous	Mo_2B_5	MoB_2 + Mo_2B_5
28	69	n. d.	2136	2240	Heterogeneous	Mo_2B_5	Mo_2B_5
29	70	n. d.	2130	2182	Heterogeneous	Mo_2B_5	Mo_2B_5
30	72		2080	2116	Heterogeneous	Mo_2B_5 + Trace MoB_{12}	Mo_2B_5 + B + MoB_{12}
31	75	74.7	1980	2018	Heterogeneous	Mo_2B_5 + Trace $MoB_{\sim 12}$	Mo_2B_5 + B + $MoB_{\sim 12}$
32	78	n. d.	1960	1990	Heterogeneous	Mo_2B_5 + Trace MoB_{12}	Mo_2B_5 + B + $MoB_{\sim 12}$
33	88	n. d.	1946	1956	Heterogeneous	Mo_2B_5 + $MoB_{\sim 12}$	n. d.

n.d. Not Determined

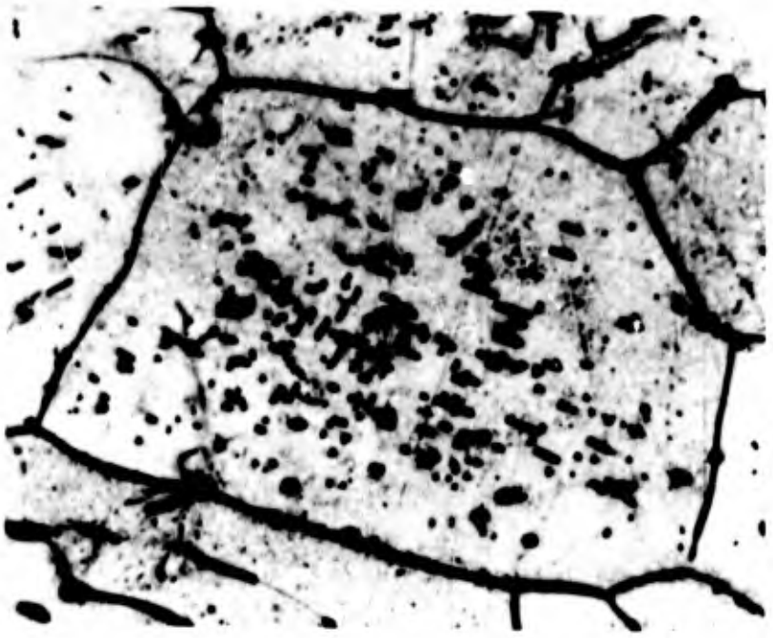

Figure 6. Mo-B (2 At% B), Rapidly Cooled from 2400°C. X1000

Primary Molybdenum with Mo_2B-Precipitations and Mo_2B at the Grain Boundaries

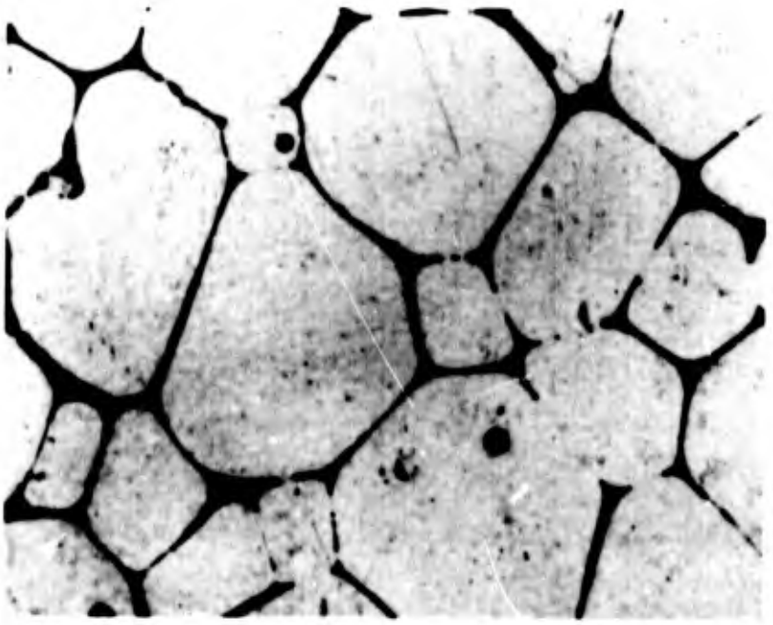

Figure 7. Mo-B (5 At% B), Cooled with Approximately 40°C per Second from 2400°C. X1000

Primary Molybdenum with Mo-Mo_2B Eutectic at the Grain Boundaries

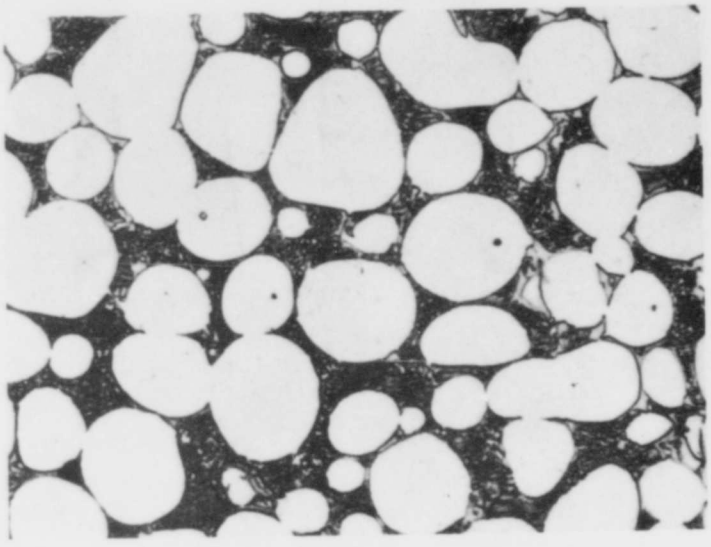

Figure 8. Mo-B (15 At% B), Rapidly Cooled from 2200°C. X1000

Primary Molybdenum in a Matrix of Mo-Mo_2B Eutectic

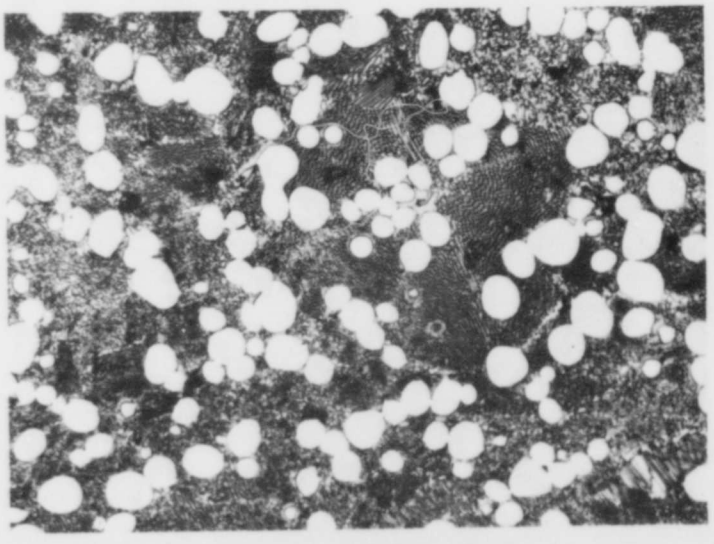

Figure 9. Mo-B (20 At% B), Rapidly Cooled from 2180°C. X500

Primary Molybdenum in a Matrix of Mo-Mo_2B Eutectic

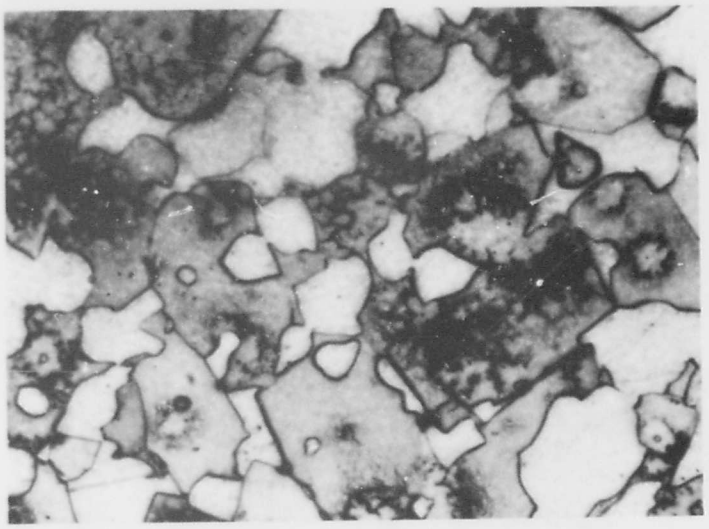

Figure 10. Mo-B (20 At% B), Sintered at 2100°C. X1000
Mo + Mo_2B

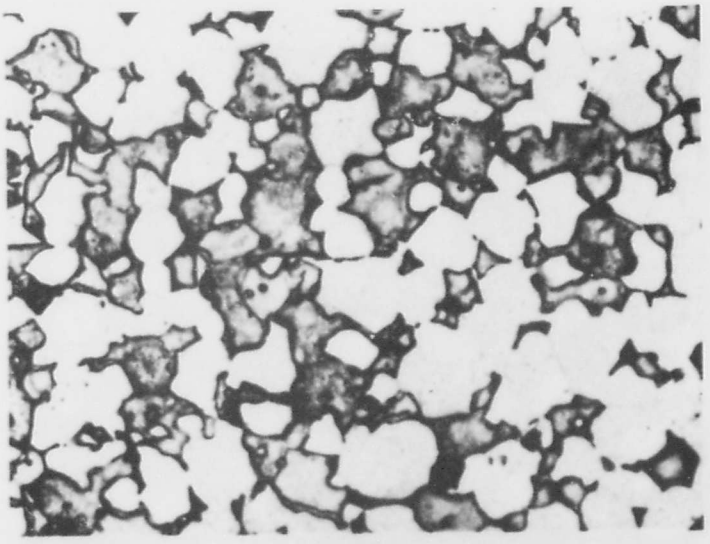

Figure 11. Mo-B (25 At% B), Sintered at 2100°C. X1500
Mo + Mo_2B

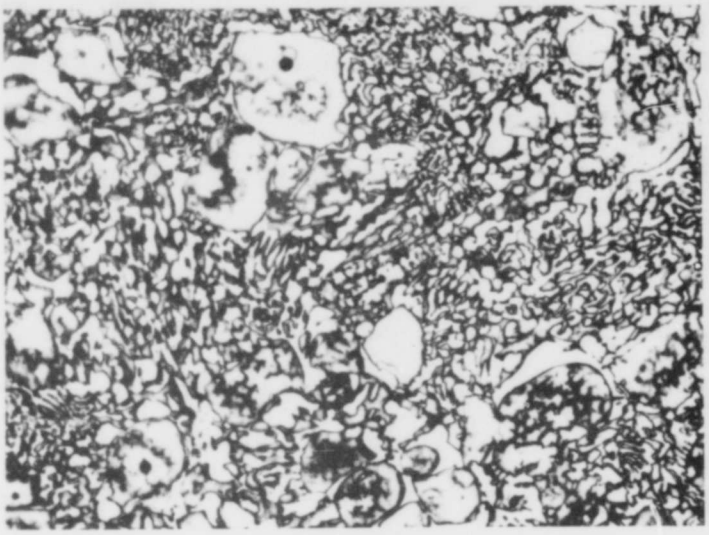

Figure 12. Mo-B (25 At% B), Rapidly Cooled with ~40°C per Second from 2180°C. X750

Primary Crystallized Mo_2B in a Matrix of Mo-Mo_2B Eutectic

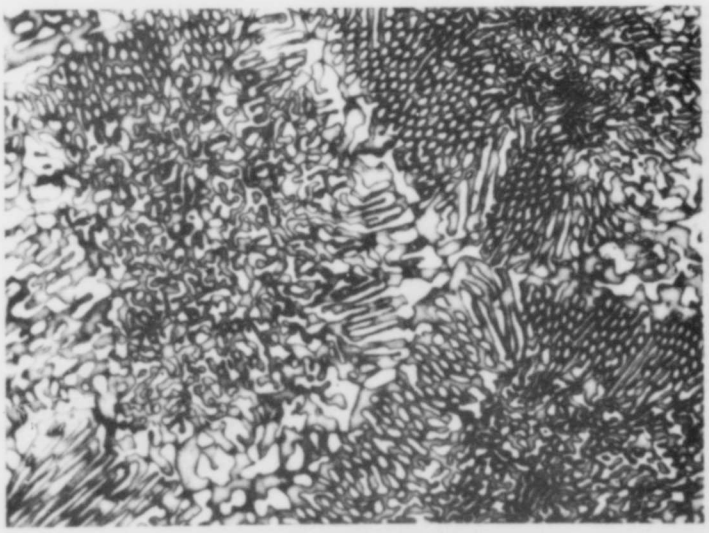

Figure 13. Mo-B (23 At% B), Rapidly Cooled from 2200°C. X1500

Mo-Mo_2B Eutectic

The eutectic structure itself is built up of a boride matrix with the molybdenum embedded in fibrillous form (Figures 14 and 15). It is interesting to note, that the morphology of the eutectic changes to a nodular-lamellar type at hypereutectic boron concentrations.

An alloy specimen with 30 At% B is still two-phased, containing small amounts of metal at the Mo_2B grain boundaries (Figure 16), while a sample with 33.4 At% B is single phase (Figure 17).

X-ray examination of the alloys up to boron concentrations of 33 At% only showed molybdenum and Mo_2B to be present in varying amounts. No precipitations from the Mo_2B-phase were noticed, and the lattice parameters showed insignificant variation only (Table 9). The homogeneity range of Mo_2B is therefore very small.

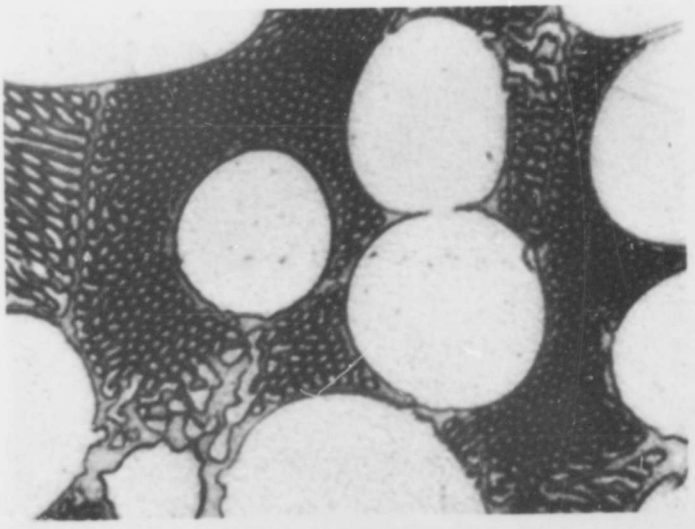

Figure 14. Mo-B (15 At% B), Rapidly Cooled from 2200°C. X2500
Primary Molybdenum and Mo-Mo_2B Eutectic.
(Note Fibrillous Molybdenum in the Eutectic Structure)

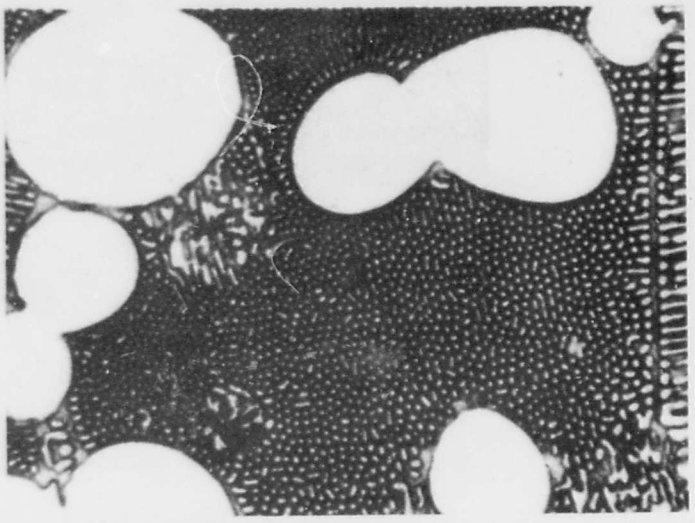

Figure 15. Mo-B (20 At% B), Rapidly Cooled From 2180°C. X2500

Primary Molybdenum and Mo-Mo_2B Eutectic
Eutectic: Fibrillous Molybdenum in a Mo_2B-Matrix

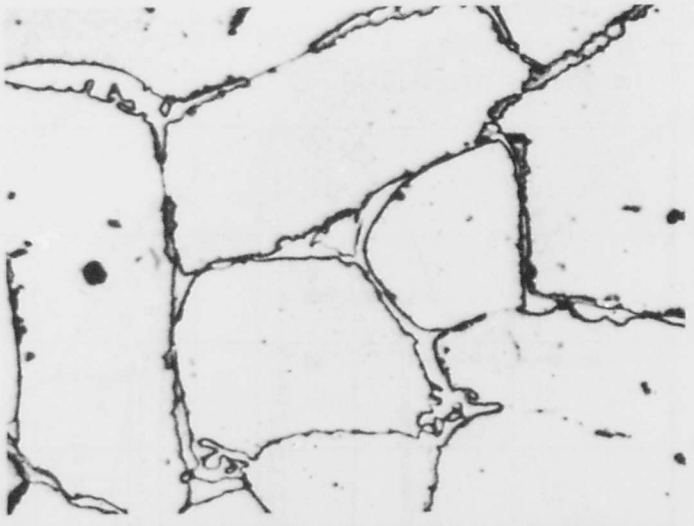

Figure 16. Mo-B (30 At% B) Rapidly Cooled from 2200°C. X1000

Primary Mo_2B with Molybdenum (Depleted Eutectic)
at the Grain Boundaries

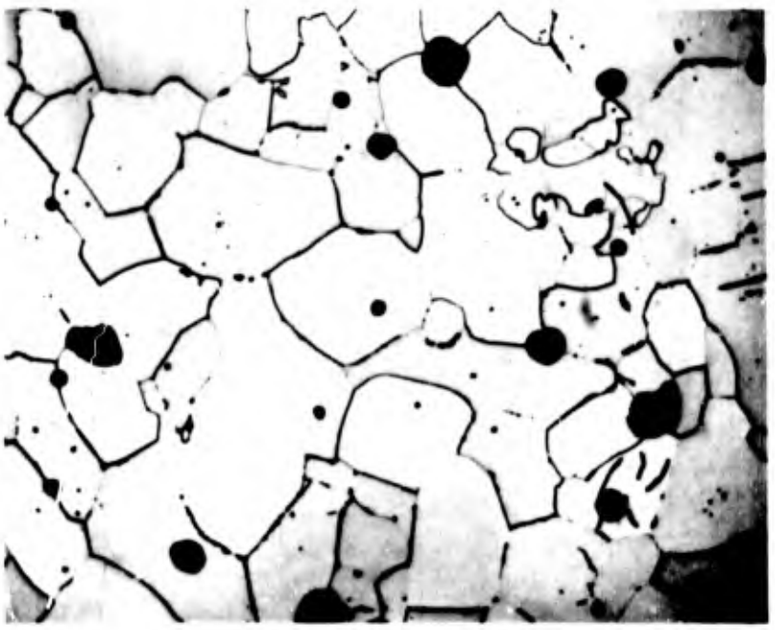

Figure 17. Mo-B (33.4 At% B), Rapidly Cooled from 2200°C. X500 Single Phase Mo_2B Pores (Black)

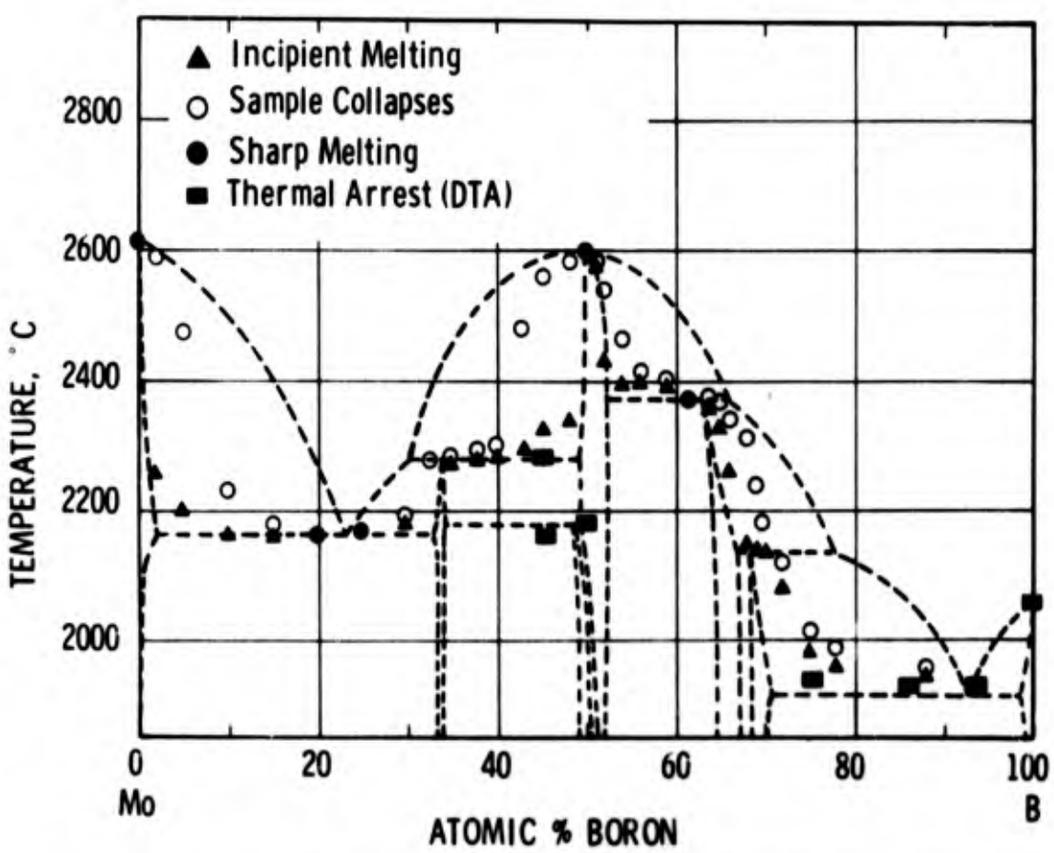

Figure 18. Melting Temperatures and Reaction Isotherms in the Molybdenum-Boron System

Table 9. Lattice Parameters of Molybdenum-Boron Phases

Concentration, At% B	Treatment	Phases Present (X-Ray)	Lattice Parameters, Angström
30	2200°C, Rapidly Cooled	Mo_2B + Trace Mo	a=5.547 Å, c=4.742 Å (Mo_2B)
35	1700°C, Slowly Cooled	Mo_2B + α-MoB	a=5.547 Å, c=4.740 Å (Mo_2B)
40	2000°C, Quenched	Mo_2B + α-MoB	a=3.103 Å, c=16.97 Å (α-MoB)
42	1700°C, Slowly Cooled	Mo_2B + α-MoB	a=3.103 Å, c=16.97 Å (α-MoB)
53	1700°C, Slowly Cooled	α-MoB+Traces MoB_2+Mo_2B_5	$a=3.113_8$ Å, $c=16.95_0$ Å (α-MoB)
43	2230°C, Quenched	Mo_2B+ β-MoB	a=3.145 Å, b=8.472 Å, c=3.063 Å (β-McB)
48	2250°C , Quenched	β-MoB	a=3.147 Å, b=8.475 Å, c=3.066 Å (β-MoB)
52	2050°C, Quenched	β-MoB	a=3.150 Å, b=8.488 Å, c=3.082 Å, (β-MoB)
61	2000°C, Quenched	β-MoB + MoB_2	a=3.044 Å, c=3.062 Å (MoB_2)
67	2000°C, Quenched	MoB_2 + Mo_2B_5	a=3.041 Å, c=3.072 Å (MoB_2) a=3.005 Å, c=21.00 Å (Mo_2B_5)
71.5	2000°C, Quenched	Mo_2B_5	a=3.012 Å, c=20.92 Å (Mo_2B_5)
91	1700°C, Slowly Cooled	$MoB_{\sim 12}$	a=3.004 Å, c=3.174 Å (MoB_{12}, Subcell)

Two-phase (heterogeneous) melting was found in all alloys with boron concentrations varying between 30 and 45 atomic percent; no break or discontinuity, which could be related to the occurrence of a compound at ~40 At% could be detected (Table 8 and Figure 18). Also, no signs of interaction between the monoboride phase

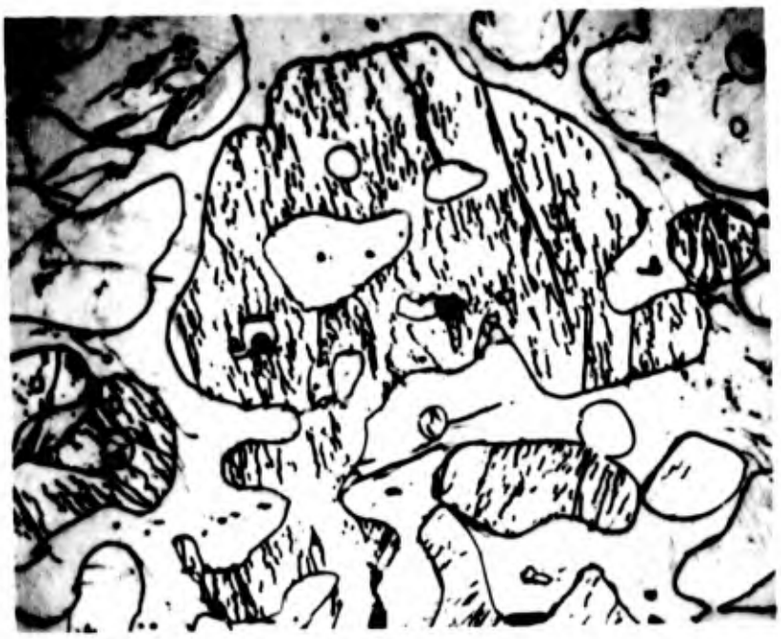

Figure 19. Mo-B (40 At% B), Cooled with ~80°C per Second from 2300°C. X500

X-ray: Mo_2B and β-MoB

The 'Measle'-Type Substructure of the MoB-Grains Could be Related to the Beginning Decomposition of the β-MoB Phase.

and Mo_2B could be found by metallographic and X-ray examination of alloys in this concentration range. Depending on the equilibrium temperature, Mo_2B was found in equilibrium with either α- or β-MoB (Figures 19 to 21).

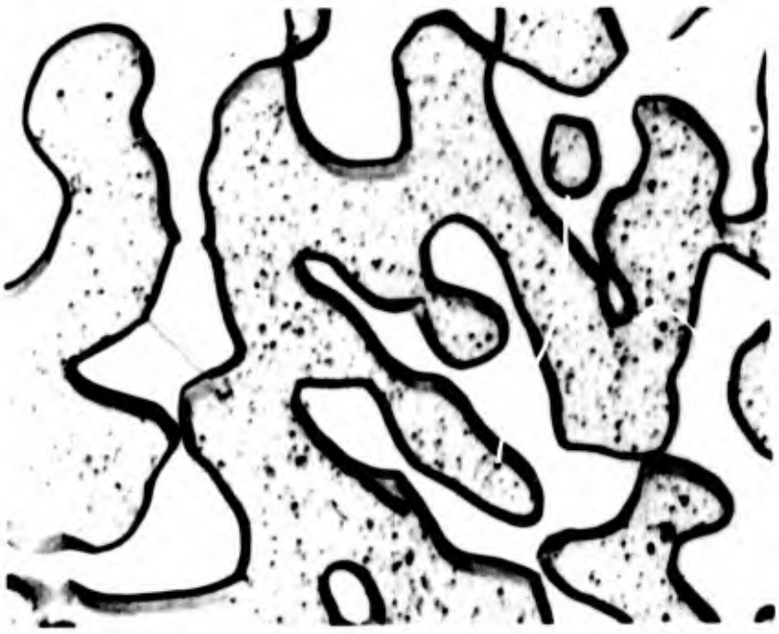

Figure 20. Mo-B (40 At% B), Melted at 2300°C, X1000
Equilibrated for 12 Minutes at 2080°C and Quenched.
X-ray: Mo_2B + α-MoB

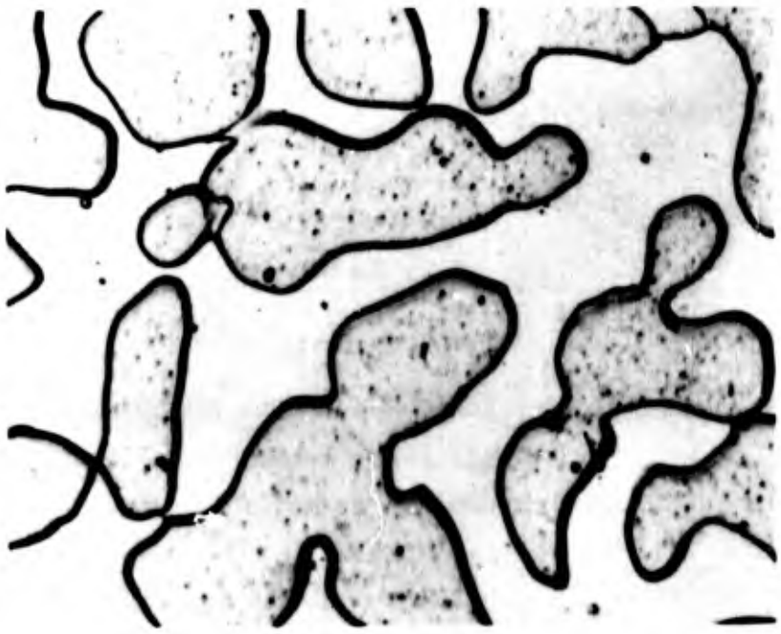

Figure 21. Mo-B (40 At% B), Melted at 2300°C, X1000
Equilibrated for 10 Minutes at 1980°C, and Quenched.
X-ray: Mo_2B + α-MoB

Differential thermoanalytical studies performed on an alloy with 44 At% B showed two thermal arrests, which are associated with the peritectic reaction at ~2300°C and the peritectoid formation (cooling) or decomposition (heating) of a α-MoB at temperatures in the vicinity of 2200°C. Based on these results, the existence of Mo_3B_2 as a true binary compound appears unlikely.

At high temperatures (2200 to 2400°C), the β-MoB phase extends from 48 to 52 At% B (Figures 22 and 23, Table 8), and melts congruently at 2600°C at a composition of ~ 50 At% B.

Figure 22. Mo-B (48 At% B), Rapidly Quenched from 2400°C. X500
Single Phase β-MoB
(Cracks are Due to Rapid Cooling)

The peritectoid reaction at 2200°C, which leads to the formation of the α-MoB-phase according to

$$Mo_2B + \beta\text{-MoB} \longrightarrow \alpha\text{-MoB}$$

Figure 23. Mo-B (52 At% B), Quenched from 2400°C. X500
β-MoB with Pores (Black)

is rapid and proceeds to completion at cooling rates below $1°C \cdot sec^{-1}$ (Figure 24). The eutectoid decomposition of β-MoB at hyperstoichiometric boron concentrations proceeds very sluggishly (Table 10).

The transformation reaction β-MoB → α-MoB proceeds by oriented nucleation and growth of the α-phase at the expense of the high temperature modification (Figures 25 to 27).

Alloys within the concentration range from 52 to 63 At% B are two-phased, and contain after quenching from temperatures above 1800°C β-MoB and MoB_2 (Figure 28). From the observed incipient melting temperatures (Figure 18, Table 8) a peritectic reaction isotherm

$$P + \beta\text{-MoB} \rightarrow MoB_2$$

at 2375°C was derived.

Table 10. Decomposition of β-MoB: X-Ray Results on Annealed Alloys

Boron Content, At%	Annealing Treatment*	Phases Present After Annealing (X-Ray)
50	Cooled with 0.5°C·sec^{-1} from 2300°C	α-MoB
51	20 hrs, 1700°C	α-MoB
52	2 hrs, 2000°C	β-MoB
	+ 12 hrs, 1900°C	β-MoB
	+ 12 hrs, 1850°C	β-MoB
	11 hrs, 1750°C	β-MoB+ Trace α-MoB(very diffuse)
	72 hrs, 1700°C	β-MoB + α-MoB
54	20 hrs, 1700°C	β-MoB + Traces α-MoB + MoB_2
	72 hrs, 1700°C	β-MoB+ α-MoB + MoB
		(α-MoB - pattern very diffuse)

*Samples were rapidly cooled from 2300°C prior to the annealing treatments, and contained the high temperature modification (β) of MoB.

DTA-runs on a sample with 63 At% B showed a weak and strongly rate dependent thermal arrest at temperatures around 1500°C. The decomposition of MoB_2 towards lower temperatures was known from previous investigations[3], and the observed thermal arrest was therefore attributed to this reaction. This assumption was confirmed in subsequent metallographic and X-ray studies on annealed specimens. The eutectoid reaction proceeds on localized crystal-planes (probably 0001) of the MoB_2-lattice. While the initial nucleation reaction proceeds with high speed, subsequent growth to larger crystallites occurs slow

(Figures 28 to 32). Annealing treatments of originally single phased MoB_2 for 2, 4, 7, and 11 hours at 1400°C still showed the diboride to be present in appreciable amounts and traces of MoB_2 were also observed in an alloy with 67 At% B after a 140 hour treatment at the same temperature.

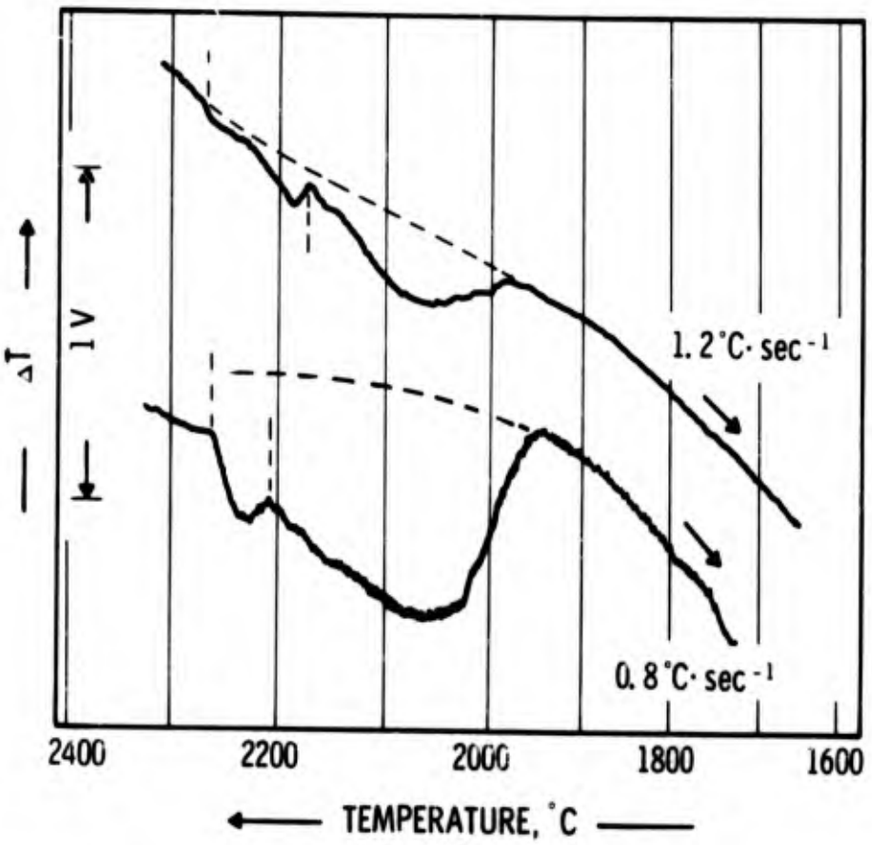

Figure 24: DTA-Thermogram (Cooling) of a Molybdenum-Boron Alloy with 47 Atomic Percent Boron.

Thermal Arrests: ~2300°C: P + β-MoB ⟶ Mo_2B

~2200°C: Mo_2B + β-MoB ⟶ α-MoB

X-Ray: $1.2°C \cdot sec^{-1}$ (top curve): α-MoB + Traces of Mo_2B and β-MoB

$0.8°C \cdot sec^{-1}$ (lower curve): α-MoB + Trace Mo_2B

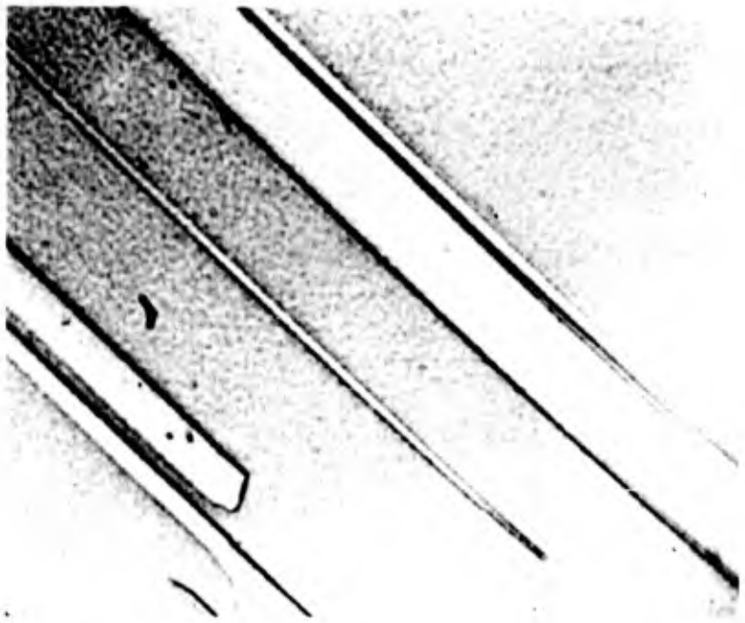

Figure 25. Mo-B (50 At% B), Cooled with 6°C per Second from 2200°C. X2500

Oriented Growth of α-MoB Nuclei in a Homogeneous Matrix of β-MoB

Figure 26. Mo-B (50 At% B), Cooled with 2°C per Second from 2200°C. X2500

Link-up of Grown α-MoB Nuclei to a Grain Boundary

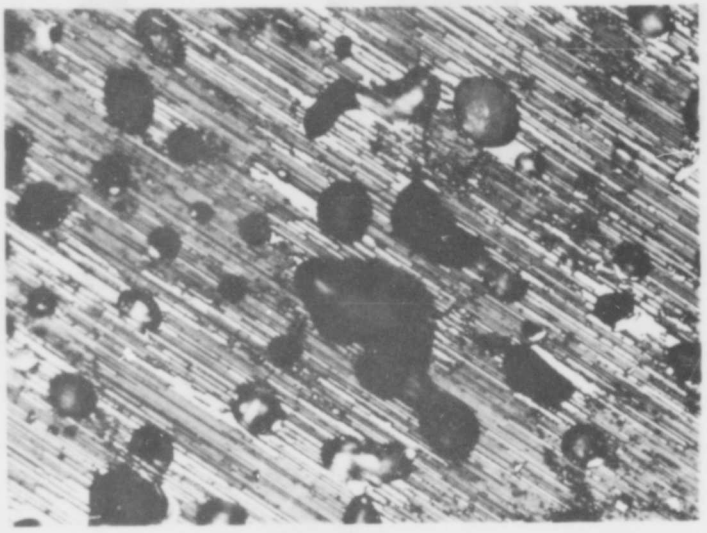

Figure 27. Mo-B (50 At% B), Cooled with 2°C per Second X750
from 2200°C.
X-ray: α-MoB with Small Amounts of β-MoB

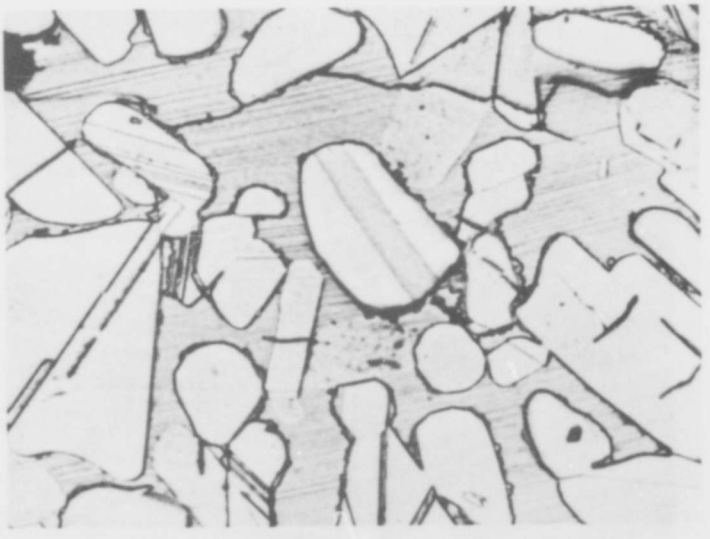

Figure 28. Mo-B (56 At% B), Cooled with ~30°C per Second X1000
from 2400°C.
β-MoB and MoB_2 (Banded)

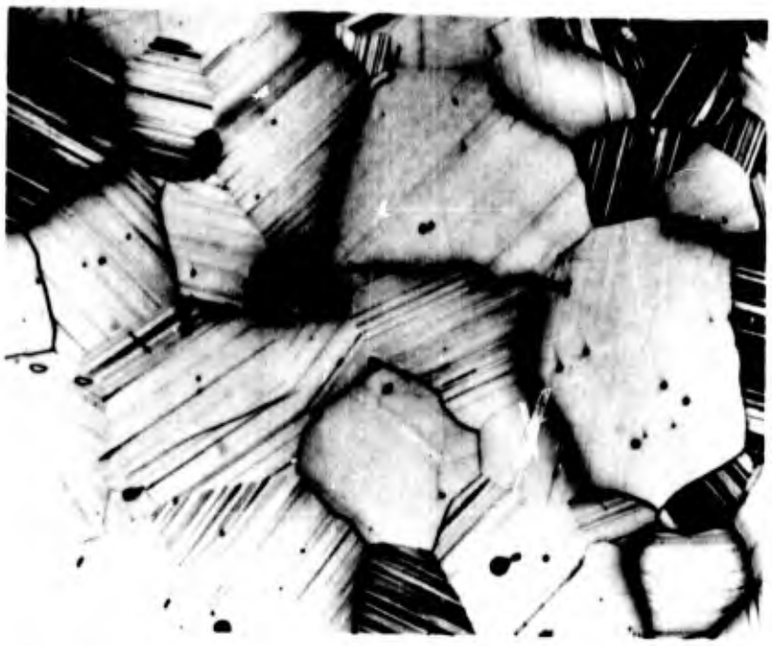

Figure 29. Mo-B (66 At% B), Cooled with ~40°C per Second X200
from 2350°C.
MoB_2 with Localized Initiation of Eutectoid Reaction.
X-ray: Single Phase MoB_2

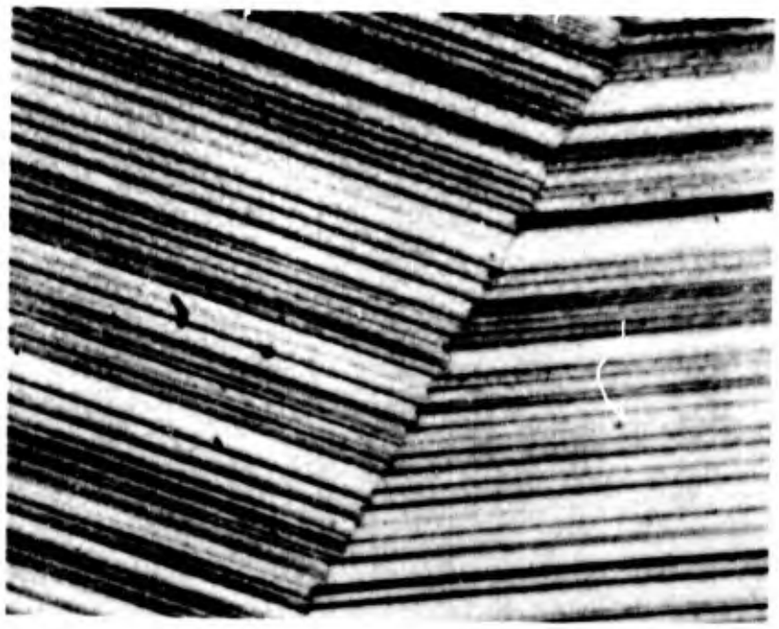

Figure 30. Mo-B (66 At% B), Cooled with ~40°C per Second X2000
from 2350°C.
Localized Nucleation of Mo_2B_5 + MoB in MoB_2

Figure 31. Mo-B (56 At% B), Rapidly Cooled from 2350°C, and Reannealed for 2 hrs. at 1400°C. X1000

X-ray: β-MoB + Trace α-MoB (Diffuse), and About Equal Amounts of MoB_2 and Mo_2B_5

Figure 32. Mo-B (56 At% B), Rapidly Cooled from 2350°C, and Reannealed for 4 hrs. at 1400°C. X1000

X-ray: β-MoB + Trace α-MoB (Diffuse) and Mo_2B_5 + MoB_2 (~70 vs 30%)

Melted alloys with 67 and 68 At% boron were two-phased, containing MoB_2 and Mo_2B_5. Alloys with 69 and 70 At% B were metallographically (Figure 33) and roentgenographically single phase Mo_2B_5, while a specimen with 72 At% B already showed excess boron, and some traces of MoB_{12}.

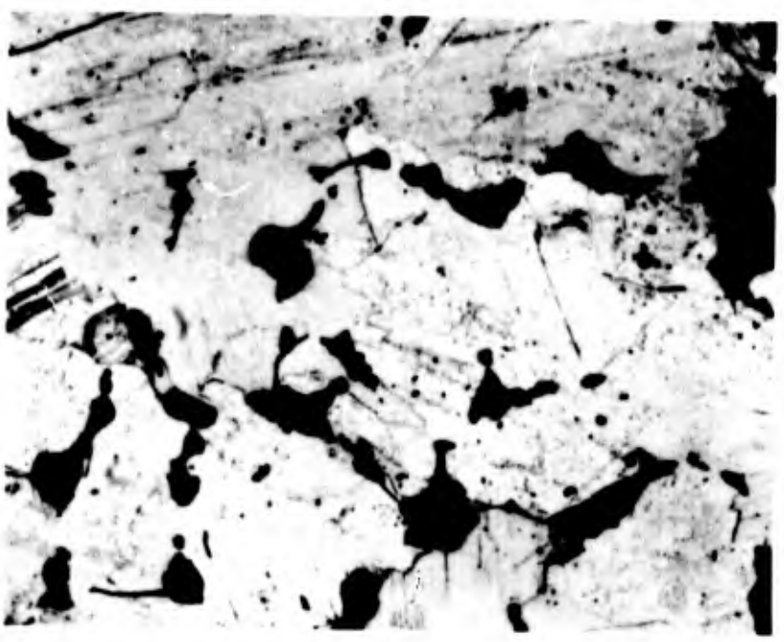

Figure 33. Mo-B (70 At% B), Rapidly Cooled from 2100°C. X750 Single Phase Mo_2B_5 Pores (Black).

Alloys in the concentration range 69-72 At% B, and which were rapidly quenched from the liquid + solid region (2150 - 2250°C), generally showed the presence of three phases: $MoB_2 + Mo_2B_5 + B$, whereas up to temperatures of 2100°C only Mo_2B_5 could be detected. Peritectic decomposition of the Mo_2B_5-phase is also suggested by the measured incipient melting temperatures, which show a slight, but definite discontinuity at temperatures of approximately 2140°C.

The boron-rich eutectic reaction isotherm was found to occur at a temperature of ~1920°C. Incipient melting in excess boron-containing alloys was difficult to observe with the Pirani-technique, since the rapidly decreasing resistivity of the alloys with temperature usually resulted in extreme high melting rates at temperatures close to melting.

A rather peculiar effect was noticed in DTA-runs with boron concentrations above 70 atomic percent: Whereas no thermal arrest could be detected in runs performed within the solidus range, a strong exotherm on the cooling cycle was noticed after the temperature of the boron-rich eutectic was exceeded in the experiments (Figure 34). The corresponding signal became weaker upon increase of the boron content (Figure 35), i.e. the generating reaction had to involve more metal-rich compositions. The reaction was absent in DTA-runs performed on pure boron. The high reaction speed observed ruled out the possibility of attributing this thermal arrest to the peritectoid formation of MoB_n ($n \sim 12$), since subsequent annealing studies showed the later reaction to proceed comparatively slow. X-ray analysis of rapidly quenched alloys (70-80 At% B, ~2200°C) showed as major constituent the diboride. A quasicontinuous change of the lattice to a type similar to that of $MoB_{\sim 12}$ was noticed in the higher boron alloys. The lattice parameters were identical with those measured previously on arc-quenched alloys[9], with the a-axis of the unit cell decreasing from 3.04 Å at 66 At% B, to 3.025 Å in excess boron-containing alloys. The c-axis increases with increasing boron content (c = 3.06 Å at 66 At% B to c = 3.12 Å). It is of interest to note, that extrapolation of these

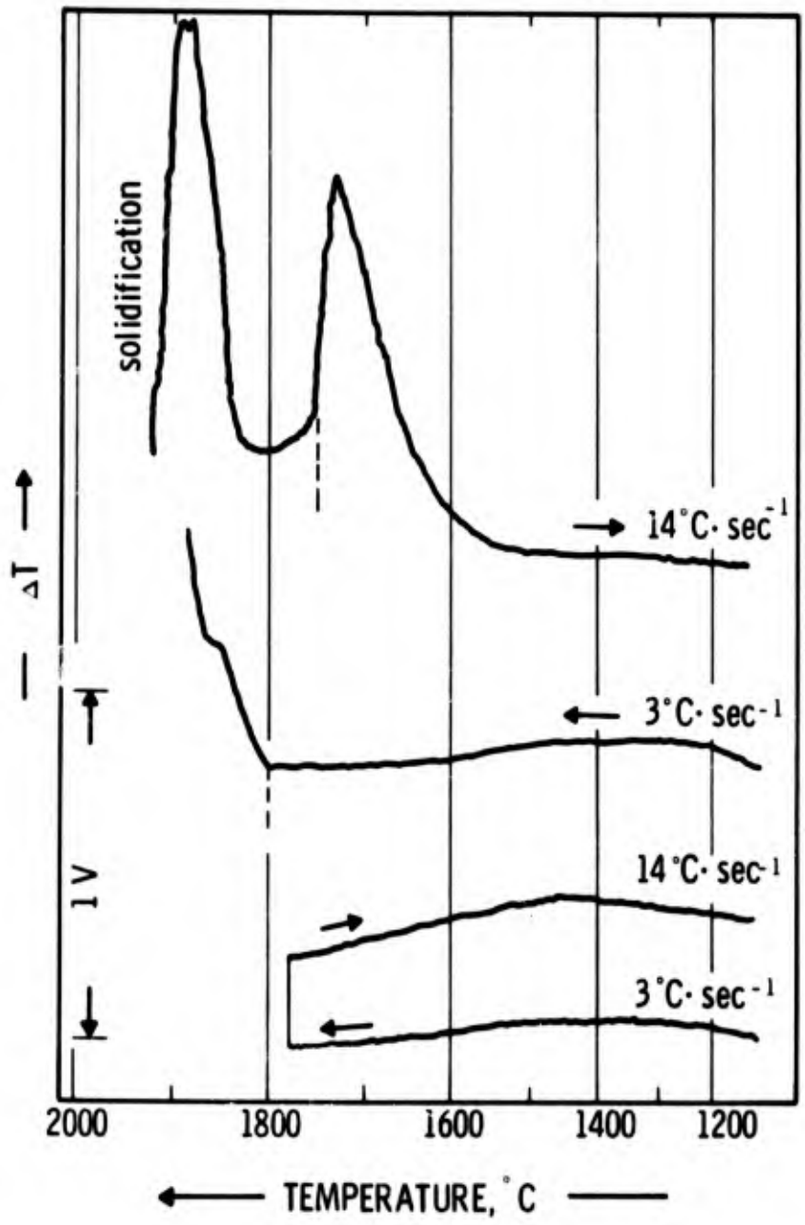

Figure 34. DTA-Thermograms of a Molybdenum-Boron Alloy with 86 Atomic Percent Boron

parameters to boron concentrations of ~90 At% (a = 3.006 Å; c = 3.17 Å) yields values, which are identical with the subcell parameters for $MoB_{\sim 12}$ (a = 3.004 Å, c = 3.174 Å).

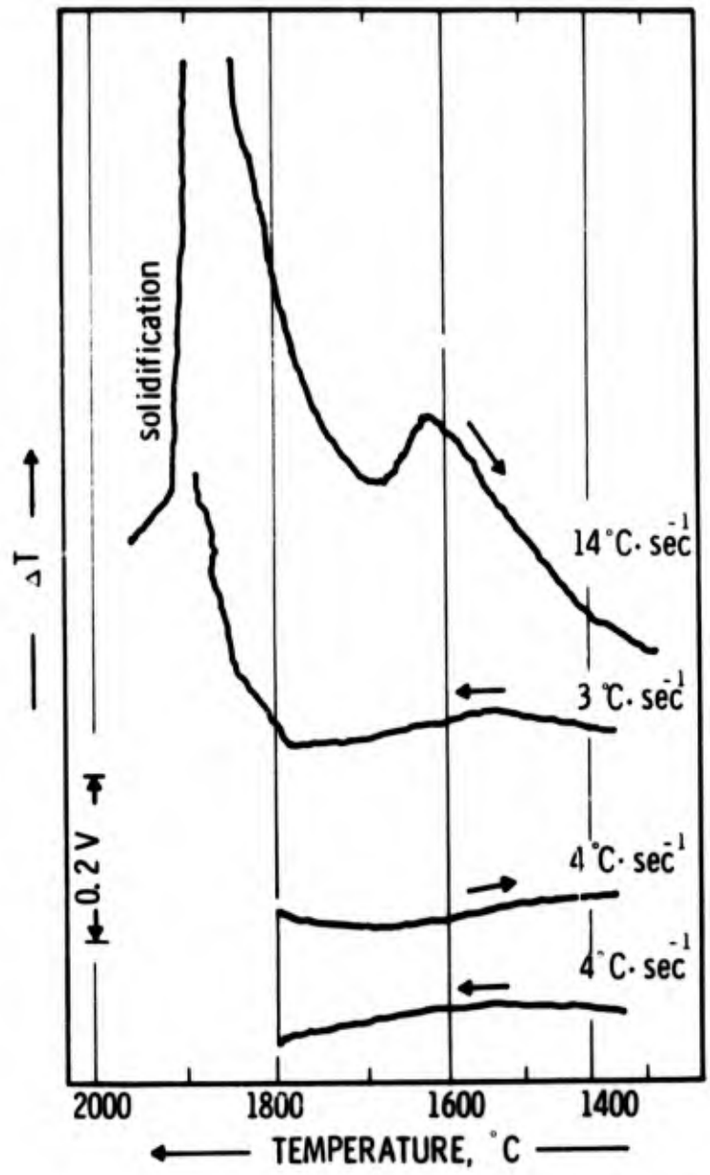

Figure 35. DTA-Thermograms of a Molybdenum-Boron Alloy with 93 Atomic % Boron

Employment of slower cooling rates (2 - 15°C per second) resulted in alloys which contained Mo_2B_5, MoB_{12}, and free boron. The results are apparently to be interpreted such, that initially, a diboride-type phase is formed in a non-equilibrium crystallization reaction from the melt, which then decomposes in a rapid solid state

reaction at temperatures of 1700 - 1800°C into a (metastable) mixture of Mo_2B_5 and boron. These reaction products then form in a comparatively slow solid state reaction the equilibrium phase $MoB_{\sim 12}$.

The temperature range of stability of the MoB_{12} phase could not be ascertained to a satisfactory degree of accuracy; metallographic examination of the alloys was only of limited use because of difficulties encountered in etching the alloys. Attempts, to differentiate the alloy phases by selective and controlled anodic oxidation, did not succeed.

High-boron alloys, heat-treated in the temperature range from 1300 to 1700°C (Figure 36), show a steady increase of the amount of MoB_{12} with increasing boron-content (72 to 90 At%), and was present in practically pure form in alloys with 90 and 92 At% B (Figure 37). At still higher boron concentration, the diffraction lines of boron were visible on the X-ray films. Alloys, heat-treated above 1800°C, were usually three-phased, containing Mo_2B_5, $MoB_{\sim 12}$, and boron. The amount of $MoB_{\sim 12}$ increased upon a preheat-treatment of the alloys at lower temperatures, but complete equilibrium was never reached. Metallographic examination of an alloy with 86 At% B, which was quenched from 1900°C, showed Mo_2B_5 and excess boron (Figure 38). The characteristic grey patches of boron gradually disappear upon heat-treatment of the alloy at lower temperatures (Figure 39), reacting with Mo_2B_5 to form the dodecarbide. An alloy with a nominal boron concentration of 93 At% shows $MoB_{\sim 12}$ and excess boron after equilibration at 1700°C (Figure 40). On the basis of the available experimental evidence, a peritectoid decomposition of MoB_{12} at subsolidus temperatures (~ 1800°C) was assumed.

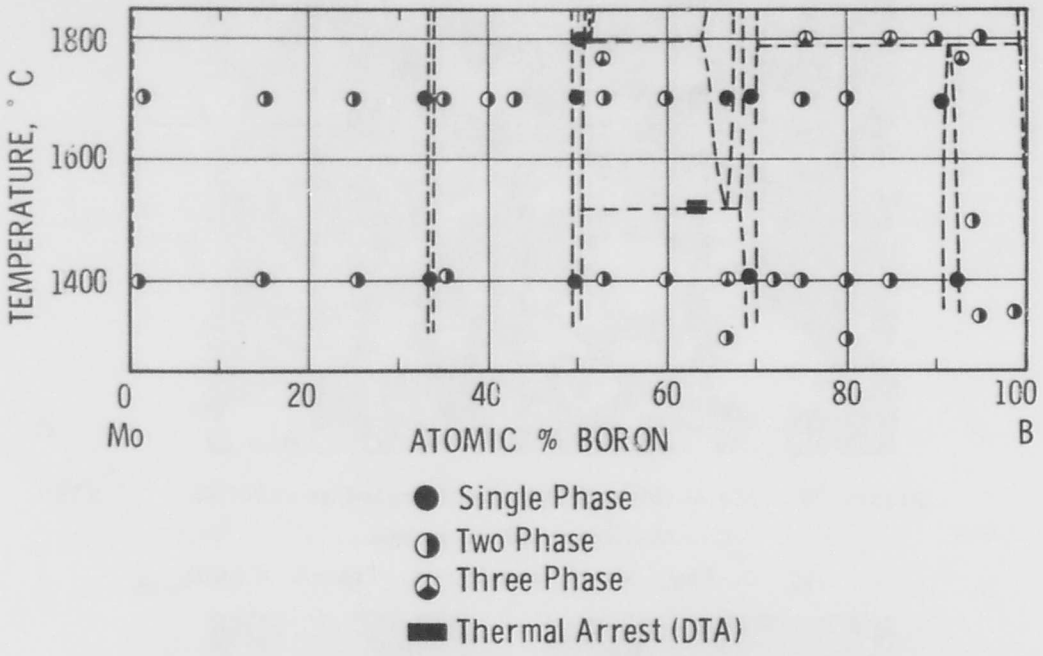

Figure 36. Molybdenum-Boron: Alloys for the Investigation of the Solid State Portion of the System

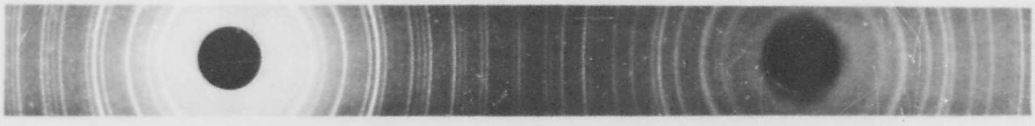

Figure 37. Powder Diffraction Pattern (Cu-K_α) of $MoB_{\sim 12}$. Alloy Mo-B (90 At% B), Heat-Treated 72 hrs at 1700°C

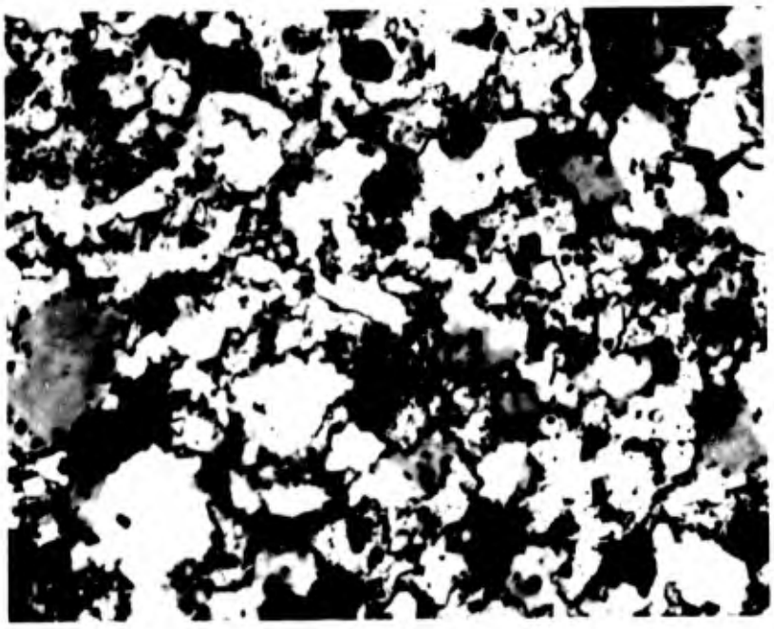

Figure 38 . Mo-B (86 At% B), Equilibrated at 1900°C. X750
After Melting, and Quenched
X-Ray: Mo_2B_5 and Boron, Traces of $MoB_{\sim 12}$

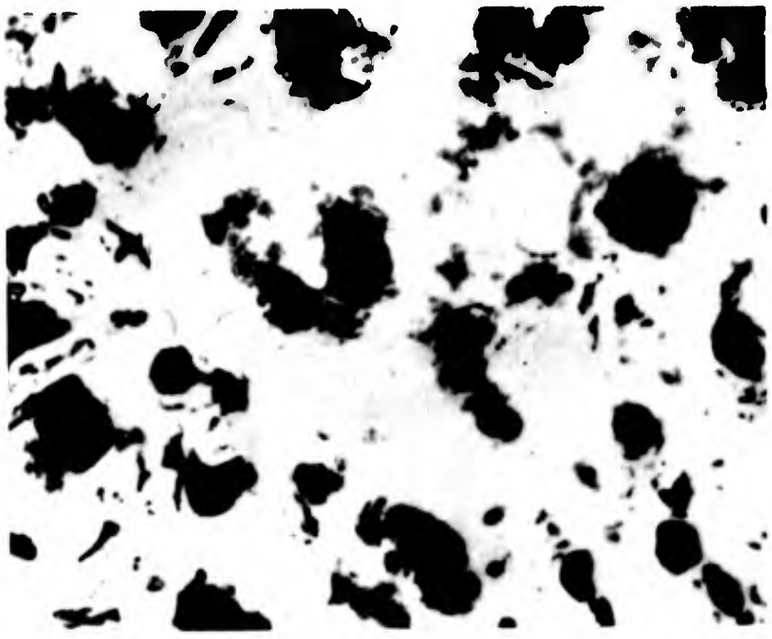

Figure 39. Mo-B (86 At% B), Sample from Figure 38 X750
Annealed at 1700°C .
Light: Mo_2B_5 Grey: Boron
Light Grey: MoB_{12} Black: Pores
X-Ray: $MoB_{\sim 12} + Mo_2B_5$

The experimental evidence gained in the investigations has been combined in the constitution diagram of the system which is shown in Figure 1.

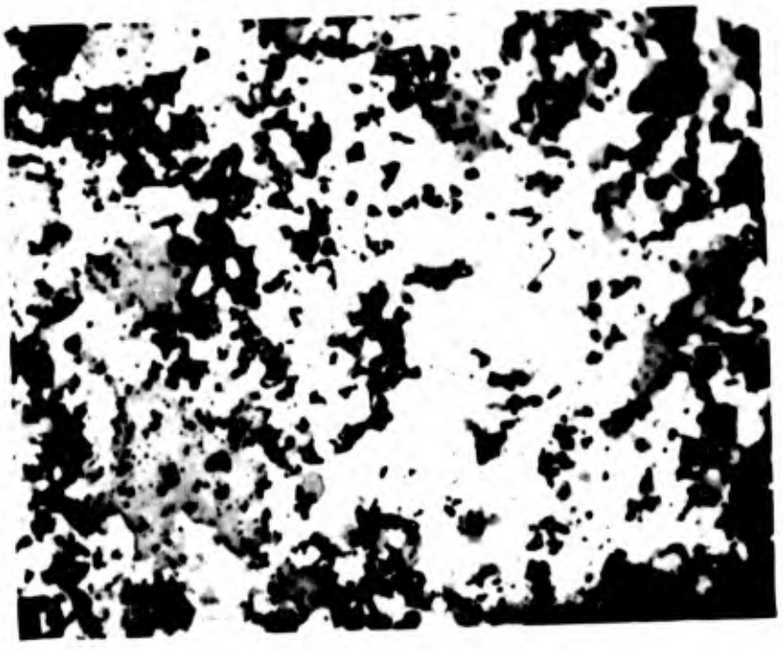

Figure 40. Mo-B (93 At% B), Equilibrated at 1700°C . X750

Light: MoB_{12}
Grey: Boron
X-Ray: $MoB_{\sim 12}$ + Boron

2. Tungsten-Boron

For pure tungsten, a melting point of 3423 ± 10°C was derived from three measurements on high-vacuum-sintered sample bars. Addition of small amounts of boron causes an extreme strong melting point depression and samples with 5 and 10 At% B are practically completely molten at temperatures of 2700 to 2800°C (Table 11, Figure 41).

Table II. Melting Temperatures of Tungsten-Boron Alloys and Qualitative Phase Evaluation After Melting

No.	At% B		Melting Temp. °C		Melting	Phases Present After Melting (X-Ray, Molten Portion)	Metallography
	Nom.	Anal.	Incipient	Collapse			
1	0	0	3423	3423	Sharp	Pure Tungsten	n.d.
2	2	n.d.	2582	3266	Heterogeneous	n.d.	W + Eutectic
3	5	n.d.	2613	2666	Heterogeneous	W + W_2B	n.d.
4	10	9	2605	2644	Slight Heterog	W + W_2B	W + Eutectic
5	14	13.5	2610	2610	Sharp	W + W_2B	W + Eutectic
6	17.5	n.d.	2612	2612	Sharp	W + W_2B	W + Eutectic
7	20	19	2600	2608	Sharp	W + W_2B	W + Eutectic
8	25	n.d.	2593	2593	Sharp	W + W_2B	W + Eutectic
9	27.5	27.3	2599	2599	Sharp	W + W_2B	Eutectic
10	30	29.4	2597	2597	Sharp	W + W_2B	W + W_2B
11	32	31.6	2602	2647	Heterogeneous	Trace W + W_2B	n.d.
12	33	n.d.	2671	2671	Sharp	Trace W + W_2B	W_2B
13	34	33.7	2668	2668	Sharp	W_2B	W_2B
14	36	n.d.	2600	2655	Heterogeneous	W_2B + α-WB	W_2B + WB
15	38	n.d.	2590	2645	Heterogeneous	W_2B + α-WB	n.d.
16	40	n.d.	2593	2604	Heterogeneous	W_2B + α-WB	W_2B + WB
17	42	n.d.	2578	2599	Heterogeneous	W_2B + α-WB + Trace β-WB	W_2B + Eutectic
18	43	n.d.	2583	2583	Sharp	W_2B + α-WB + Trace β-WB	Largely Eutectic
19	44	n.d.	2576	2586	Slightly Heterog	W_2B + β-WB	WB + Eutectic
20	46	n.d.	2572	2634	Heterogeneous	W_2B + β-WB + α-WB	n.d.
21	48	48.2	2665	2665	Sharp	β-WB + Trace α-WB	WB
22	49	n.d.	2666	2663	Sharp	β - WB	WB

Table 11. (continued)

No.	At% B Nom.	At% B Anal.	Melting Temp. °C Incipient	Melting Temp. °C Collapse	Melting	Phases Present After Melting (X-Ray, Molten Portion)	Metallography
23	50	n.d.	(2547)	2655	Fairly Sharp	α-WB + Little β-WB	WB
24	53	52.3	2536	2622	Heterogeneous	α-WB + Trace β-WB	WB + Trace W_2B_5
25	55	n.d.	2352	2440	Heterogeneous	α-WB + W_2B_5	WB + Eutectic
26	58	n.d.	2337	2383	Slightly Heterog	α-WB + W_2B_5	n.d.
27	61	n.d.	2337	2367	Slightly Heterog	α-WB + W_2B_5	WB + Eutectic
28	64	n.d.	2337	2337	Sharp	α-WB + W_2B_5	W_2B_5 + Eutectic
29	66	66.1	2337	2348	Fairly Sharp	Trace α-WB + W_2B_5	W_2B_5 + Eutectic
30	68	n.d.	2366	2366	Sharp	W_2B_5	W_2B_5
31	70	n.d.	(2285)	2365	Fairly Sharp	W_2B_5	W_2B_5 + Trace(B-$WB_{\sim 12}$)
32	71	70.7	2270	(2327)	Heterogeneous	W_2B_5	n.d.
33	73	n.d.	2280	2337	Heterogeneous	W_2B_5	W_2B_5 + B + ($WB_{\sim 12}$)
34	74	73.8	2240	2310	Heterogeneous	W_2B_5	n.d.
35	75	n.d.	2000	2130	Heterogeneous	W_2B_5 + Trace $WB_{\sim 12}$	W_2B_5 + B (+$WB_{\sim 12}$)
36	77	n.d.	2152	2203	Heterogeneous	W_2B_5 + Trace $WB_{\sim 12}$	W_2B_5 + B (+ $WB_{\sim 12}$)
37	78	n.d.	2017	2058	Heterogeneous	W_2B_5 + Little $WB_{\sim 12}$	n.d.
38	80	n.d.	(2000)	2047	Heterogeneous	W_2B_5 + $WB_{\sim 12}$	n.d.
39	84	n.d.	2008	2037	Heterogeneous	W_2B_5 + $WB_{\sim 12}$	W_2B_5 + B (+ $WB_{\sim 12}$)
40	86	n.d.	2014	2080	Heterogeneous	W_2B_5 + $WB_{\sim 12}$	W_2B_5 + B + $WB_{\sim 12}$
41	87						
42	90						
43	92						
44	95						
45	97						

Electrical Conductivity too Low for Measurement in the Pirani-Furnace

n.d. - Not Determined

The solubility of boron in tungsten is very low. A sample with 2 At% B, quenched from temperatures above the W-W_2B reaction isotherm, already shows significant amounts of eutectic (Figure 42). No

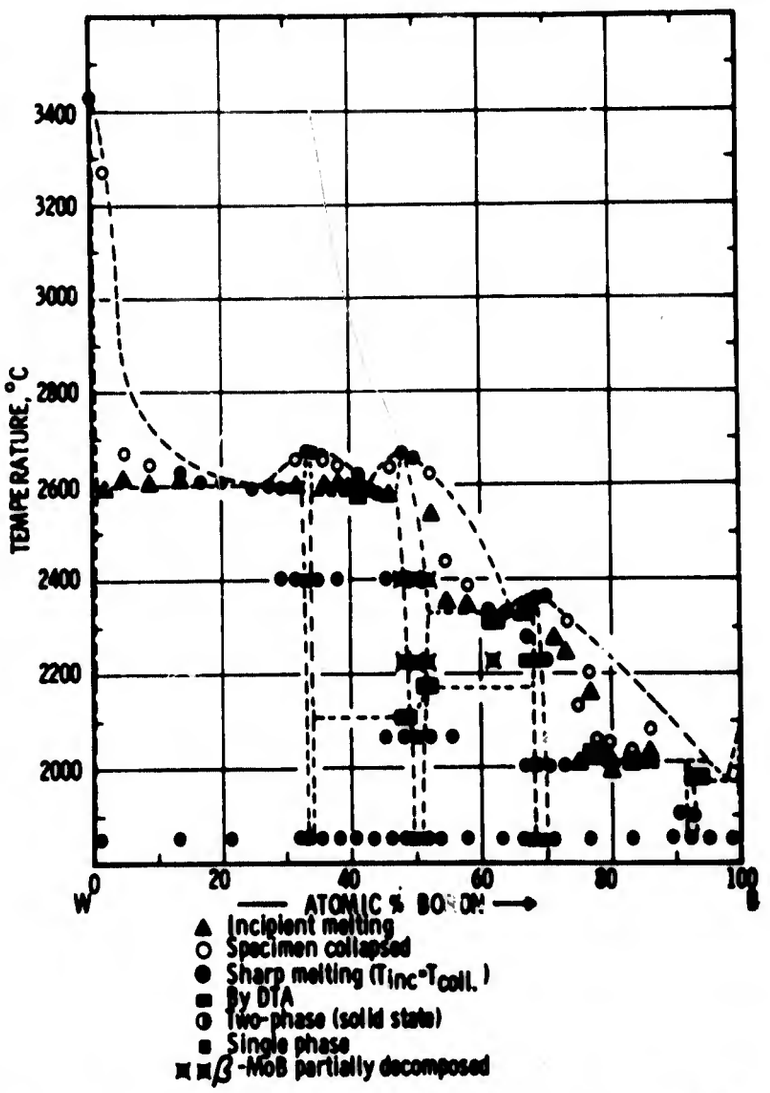

Figure 41. W-B: Melting Temperatures, DTA-Results and Qualitative Evaluation of Solid State Samples. Quenched Alloys

boride precipitations in tungsten, which would indicate a temperature-dependent boron solubility, were observed.

Figure 42. W-B (2 At% B), Quenched (~90°C · sec^{-1}) from 3270°C. X1000

Primary Tungsten with W-W_2B Eutectic at the Grain Boundaries

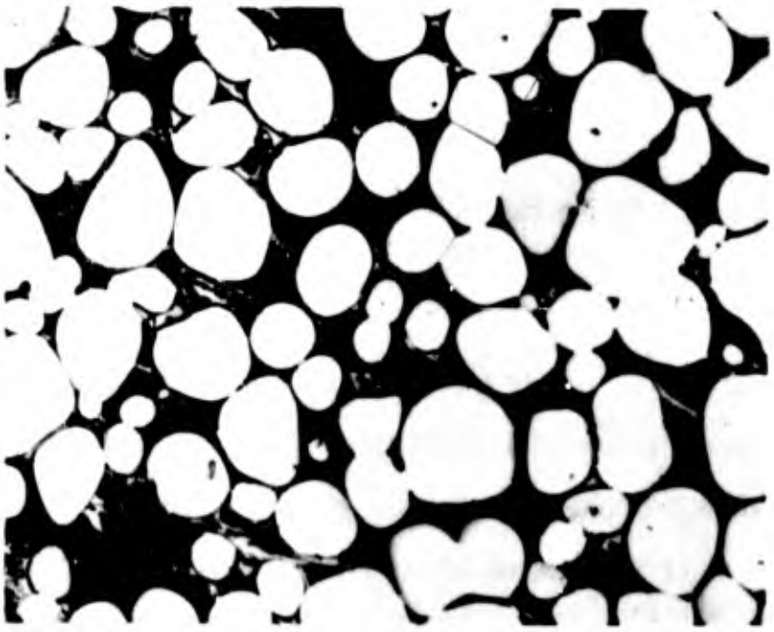

Figure 43. W-B (13.5 At% B), Cooled with ~80°C per Second from 2620°C . X1000

Primary Tungsten in a Matrix of W-W_2B Eutectic

Alloys from the concentration range 2-32 At% B are two-phased, containing W and W_2B. From the melting temperature determinations (Table 11) as well as metallographic examinations of melted and quenched alloys (Figures 43 to 51), the eutectic point of the equilibrium W-W_2B

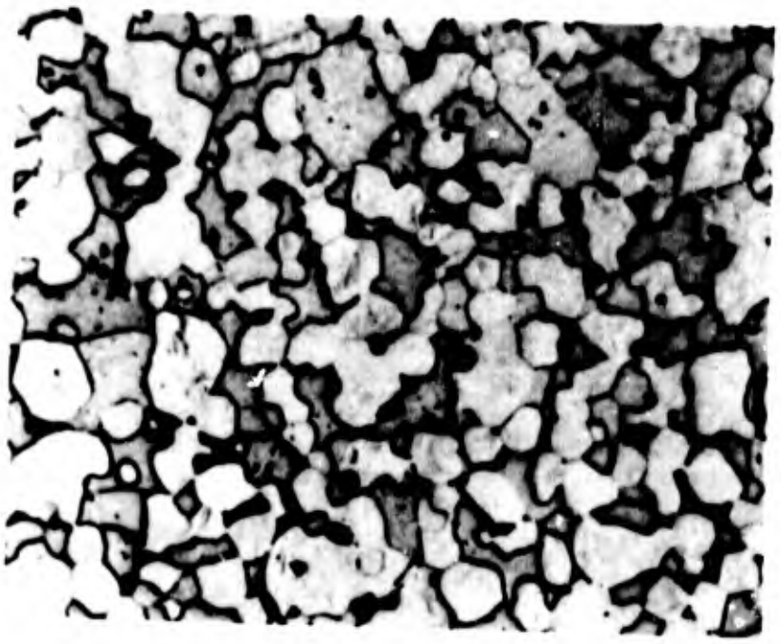

Figure 44. W-B (13.5 At% B), Sinterstructure, 2400°C. X1000
W + W_2B

was located at 2600°C and 27 At% B (Figure 2). The eutectic structure itself consists of "primary" crystallized, fibrillous tungsten, embedded in a matrix of W_2B (Figures 52 and 53).

The W_2B homogeneous range extends from approximately 33 to 34 At% B. Precipitation of WB from W_2B indicates the W_2B-WB boundary to be slightly temperature dependent (Figure 54). The variation of the lattice parameters over the homogeneity range is small (Table 12).

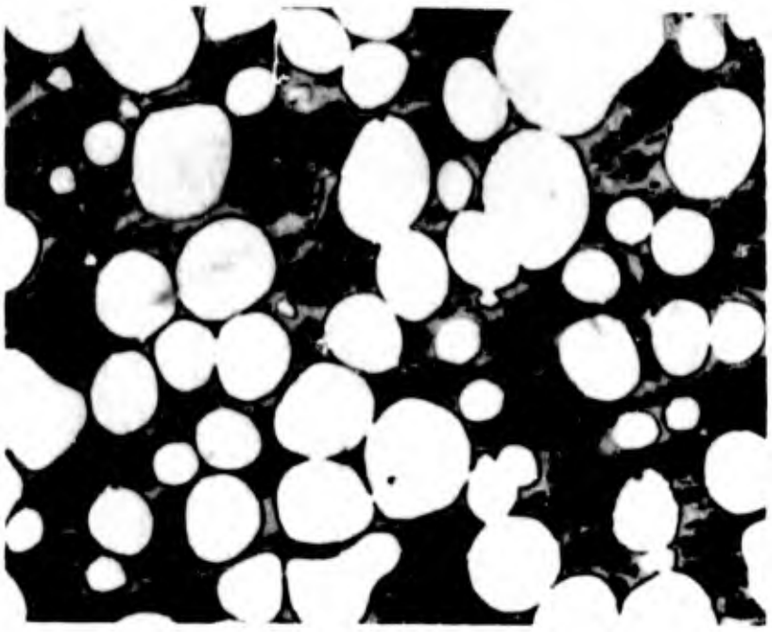

Figure 45. W-B (19 At% B), Cooled With ~80°C per Second X1000
from 2620°C.
Primary Tungsten in a Matrix of W-W_2B Eutectic

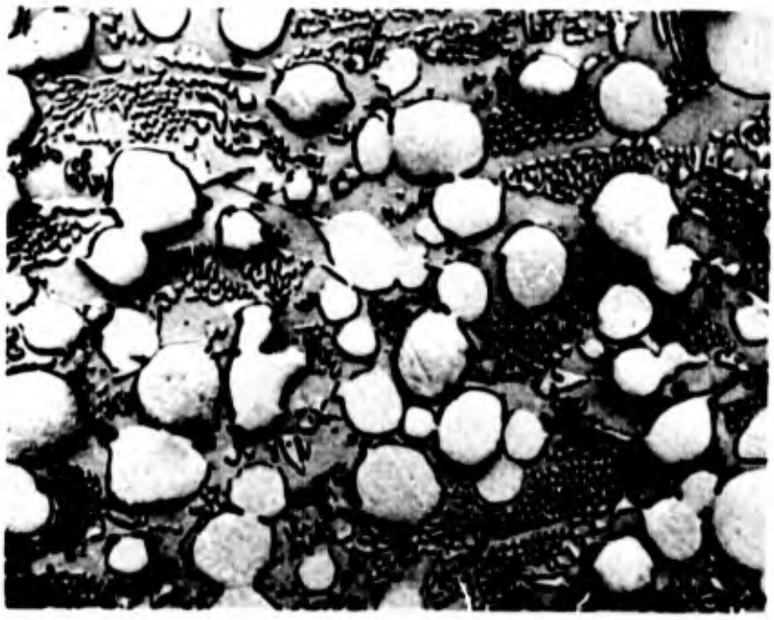

Figure 46. W-B (23 At% B), Cooled with ~70°C per Second X1000
from 2620°C.
Primary Tungsten in a Matrix of W-W_2B Eutectic

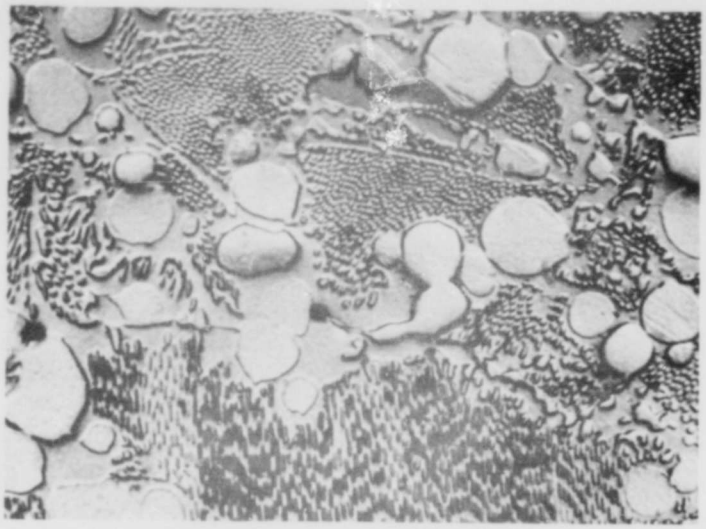

Figure 47. W-B (25 At% B), Cooled with ~80°C per Second X1000
from 2610°C.
Primary Tungsten and W-W_2B Eutectic

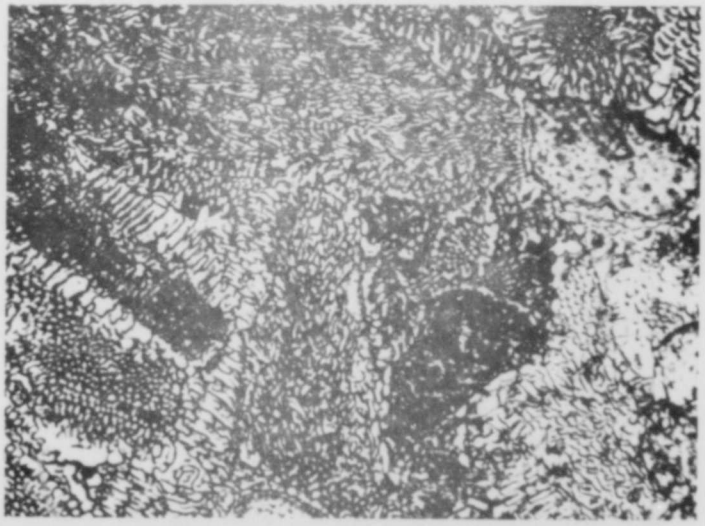

Figure 48. W-B (27.3 At% B), Cooled with ~60°C per Second X1000
from 2600°C.
W-W_2B Eutectic

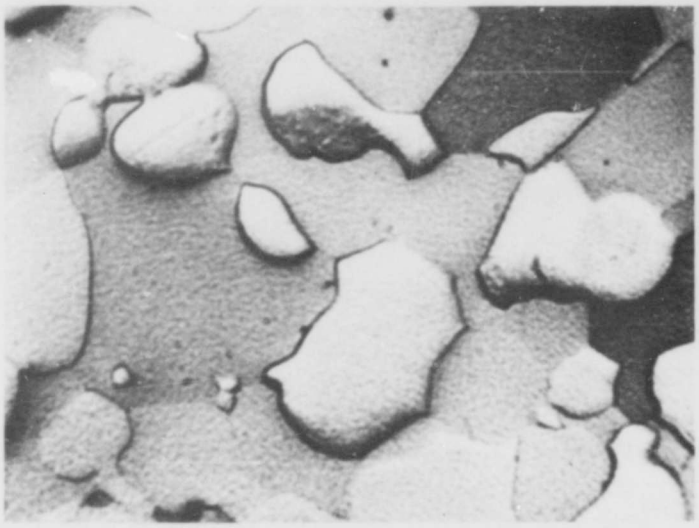

Figure 49. W-B (27.3 At% B), Rapidly Cooled from 2570°C. X2500
Sinterstructure W-W_2B

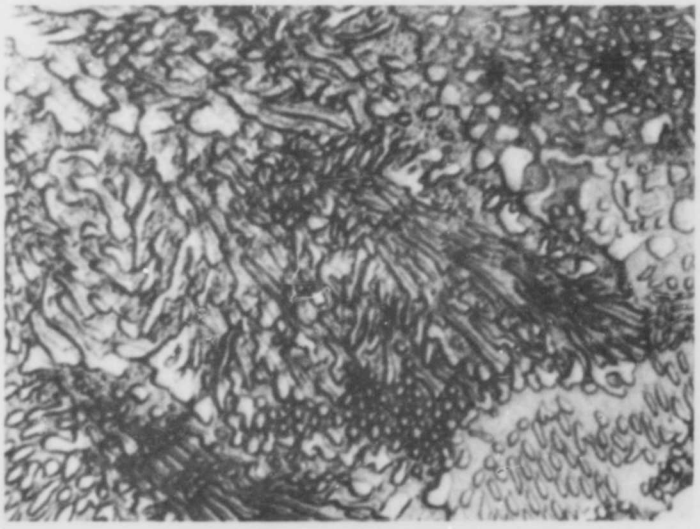

Figure 50. W-B (27.8 At% B), Cooled with ~20°C per Second from 2600°C. X2000
Traces of Binary W_2B in a Matrix of W-W_2B Eutectic

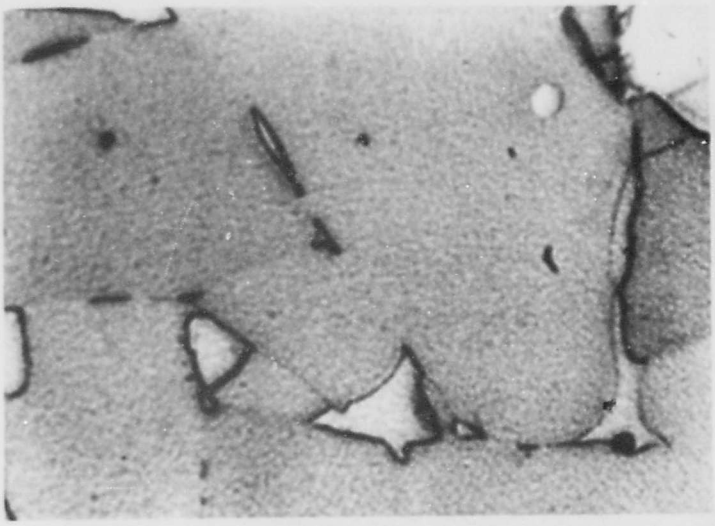

Figure 51. W-B (31.6 At% B), Cooled with ~20°C per Second from 2650°C. X2000

W_2B with Tungsten (Depleted W-W_2B Eutectic) at the Grain Boundaries

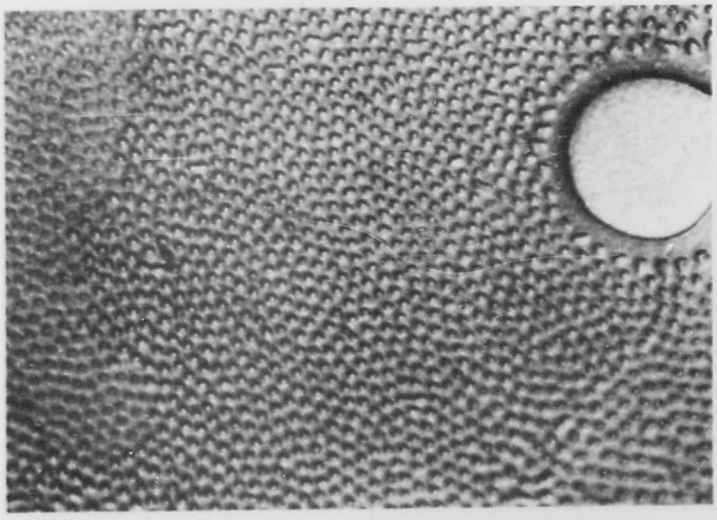

Figure 52. W-B (26 At% B), Cooled with Approximately 100°C per Second from 2610°C . X2500

W-W_2B Eutectic Structure: Fibrillous Tungsten (Light) in a Continuous Matrix of W_2B

Note the tungsten depleted zone around the primary tungsten crystal (lower left), which is approximately of the same width as the average distance between the tungsten fibrillae.

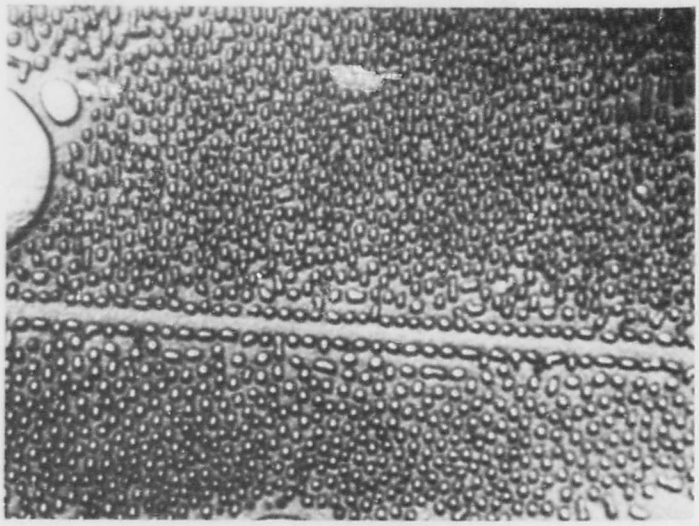

Figure 53. W-B (26 At% B), Cooled with Approximately 100°C per Second from 2610°C. X2500

W-W_2B Eutectic Structure: 'Grain-Boundary' Between Two Eutectic Colonies of Slightly Different Orientation

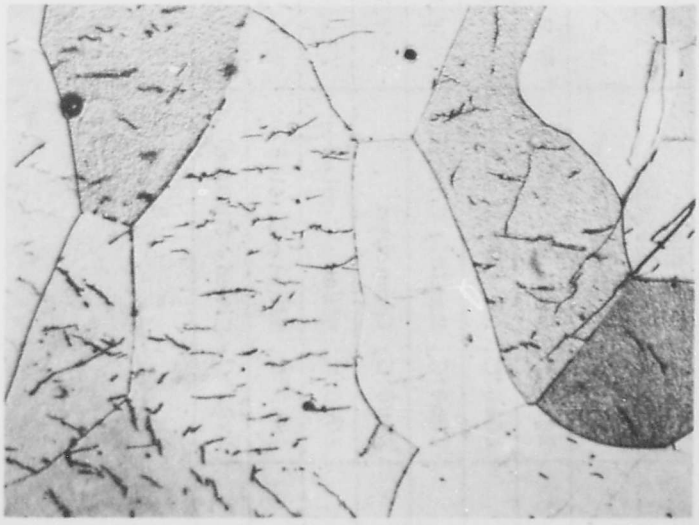

Figure 54. W-B (34 At% B), Cooled with ~60°C per Second from 2600°C. X500

W_2B with Traces of WB-Precipitations

Table 12. Lattice Parameters of Tungsten-Boron Phases

Concentration, At% B	Treatment	Phases Present (X-Ray)	Lattice Parameters, Angstrom
29	2400°C, Rapidly Cooled	W + W_2B	a=5.570 Å, c=4.744 Å, (W_2B)
38	2400°C, Rapidly Cooled	W_2B + α-WB	a=5.572 Å, c=4.746 Å, (W_2B)
48	2060°C, Rapidly Cooled	Trace W_2B+α-WB	a=3.093 Å, c=16.99$_6$ Å, (α-WB)
55	2060°C, Rapidly Cooled	α-WB + W_2B_5	a=3.120 Å, c=16.99$_2$ Å, (α-WB)
46	2400°C, Quenched	β-WB + W_2B	a=3.142 Å, c=8.506 Å, c=3.065 Å, (β-WB)
67	2000°C, Slowly Cooled	Trace α-WB+W_2B_5	a=2.980$_5$ Å, c=13.87$_9$ Å (W_2B_5)
77	1850°C, Slowly Cooled	W_2B_5 + $WB_{\sim 12}$	a=2.985$_9$ Å, c=13.90$_2$ Å (W_2B_5)
91	1900°C, Slowly Cooled	$WB_{\sim 12}$	a=3.995 Å, c=3.174 Å ($WB_{\sim 12}$, hex.Subcell)

Figure 55. W-B (42 At% B), Cooled with ~60°C per Second from 2600°C. X1000

Primary W_2B, and W_2B-β-WB Eutectic

Figure 56. W-B (43 At% B), Cooled with ~60°C per Second from 2590°C. X1000

W_2B - β-WB Eutectic (Structure not Completely Developed)

Alloys from the composition range 34 to 47 At% are two-phased, and show, depending on the chosen equilibrium temperature and the cooling conditions, either the equilibrium pair — W_2B — α-WB, or W_2B — β-WB.

From the melting temperatures of the alloys in this concentration (Table 11), together with microscopic examinations of the melted and quenched alloys (Figures 55 to 57), the eutectic point of the equilibrium β-WB-W_2B was located at 2580°C and a boron concentration of approximately 43 At%.

Recrystallization of the eutectic occurs extremely fast, and employment of cooling rates below 30°C per second generally resulted in structures, where the eutectic part was depleted in the primary crystallising component. Due to the shorter diffusion path involved in this effect, this effect is especially pronounced in alloys with compositions close to the homogeneity limits of either one of the participant phases (Figure 58). Non-uniform attack of the etchants presented a problem, and resulted in partly unresolved microstructures.

The monoboride phase melts congruently at 2665°C at a composition of 48 At% B. At ~2400°C the phase is homogeneous between approximately 48 and 52 At% B (Table 11).

The high temperature (β) modification transforms in a rapid solid state reaction into α-MoB. The transformation temperature, i.e. the α-WB temperature where the decomposition or reaction initiates, is slightly dependent on the boron concentration. In the average, temperatures of 2100°C were obtained for the eutectoid reaction isotherm

$$\beta\text{-WB} \;\text{—}\; \alpha\text{-WB} + W_2B,$$

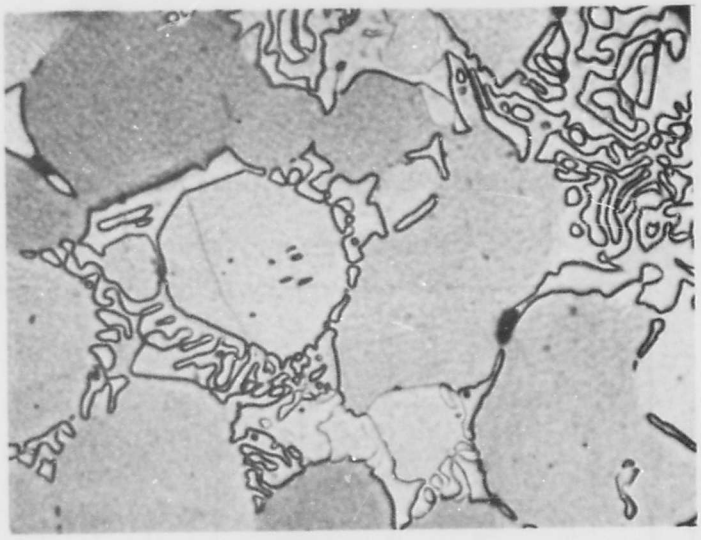

Figure 57. W-B (44 At% B), Cooled with ~80°C per Second from 2590°C. Primary WB in W_2B-WB Eutectic X1000

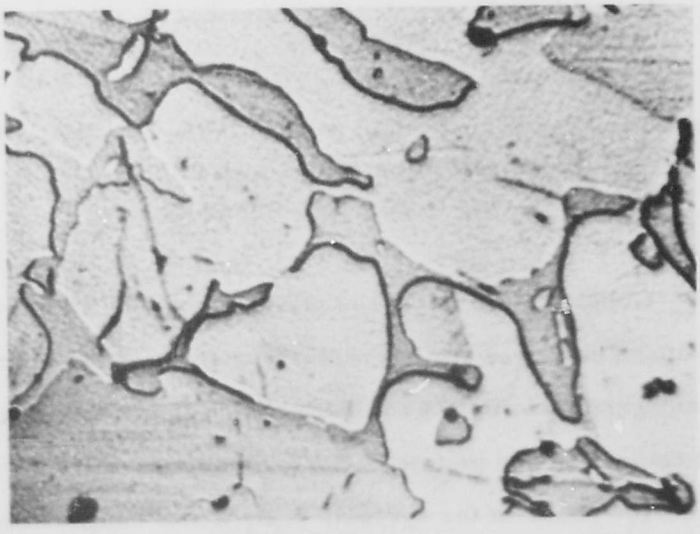

Figure 58. W-B (40 At% B), Cooled with ~20°C per Second from 2600°C. W_2B in a Matrix of WB (W_2B-Depleted Eutectic) X1000

and 2170°C for the peritectoid reaction

$$\alpha\text{-WB} \;\longrightarrow\; \beta\text{-WB} + W_2B$$

occurring at hyperstoichiometric concentrations. Reproductions of typical recorder traces are shown in Figure 59.

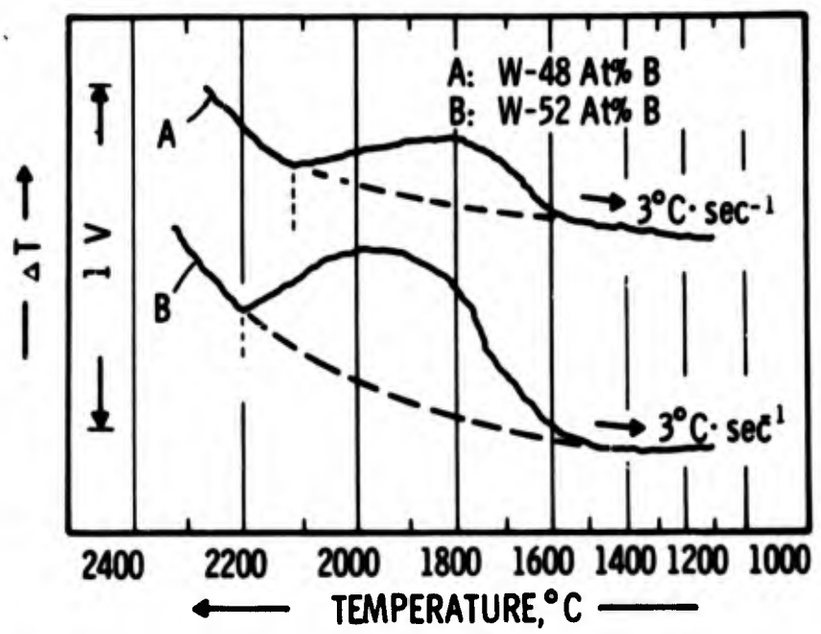

Figure 59. Decomposition of β-WB: DTA-Thermograms of Tungsten-Boron Alloys with 48 (Top Curve) and 52 (Lower Curve) At% Boron

Cooling rates in excess of 40°C per sec. are required in order to retain the β-modification in any appreciable quantity. Transformation within the homogeneous range of the monoboride is two-phased, proceeding by localized nucleation and growth of the α-modification (Figure 60). The next higher boride phase in the system, W_2B_5 melts congruently at 2365 + 10° at a boron concentration of ~68 At% (Table 11). It forms a eutectic equilibrium with β-WB at ~2340°C. From an inspection of the

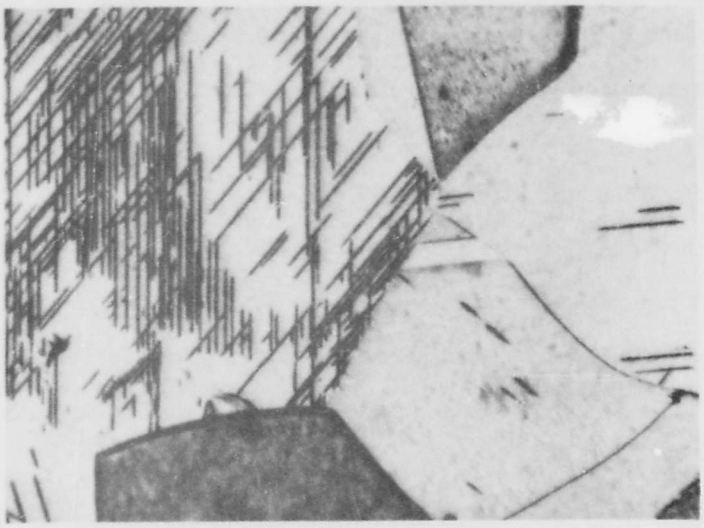

Figure 60. W-B (50 At% B), Cooled with ~100°C per Second from 2500°C. X1500

β-WB with Localized Precipitations of α-WB.

X-Ray: β-WB

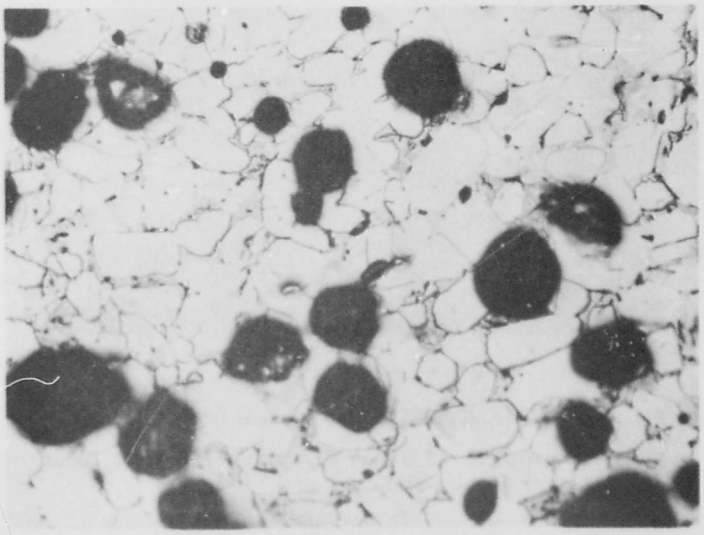

Figure 61. W-B (55 At% B), Cooled with ~40°C per Second from 2450°C. X500

Primary β-WB (Completely Transformed) in a Matrix of WB-W_2B_5 Eutectic. Pores (Black)

X-Ray: α-WB + W_2B_5

microstructures of melted and quenched alloys (Figures 61 to 64), the eutectic concentration was bracketed to within the concentration limits 63 $\pm$ 1 At% B.

While the alloy with 68 At% B is single phased (Figure 65), a sample with ~70 At% boron already shows scant traces of excess boron and $WB_{\sim 12}$ at the grain boundaries (Figure 66). The lattice parameters of W_2B_5 show only a very nominal change with the boron concentration (Table 12). The peritectic decomposition of the high-boron phase ($WB_{\sim 12}$)

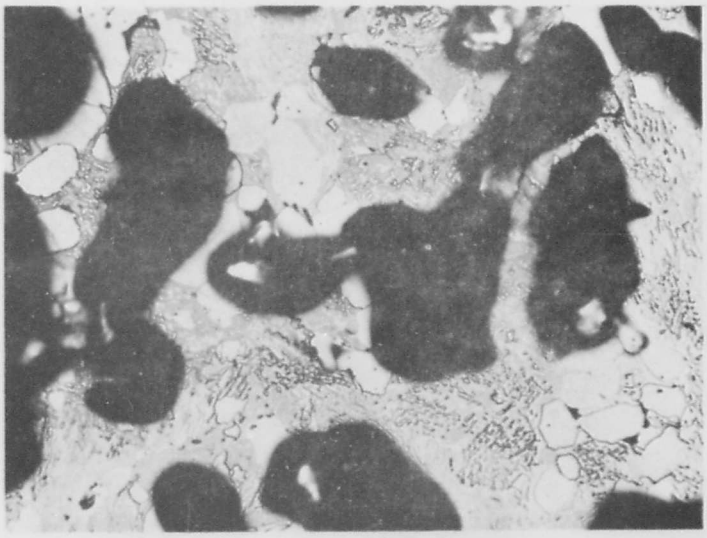

Figure 62. W-B (62 At% B), Quenched from 2350°C. X500
Small Amounts of Binary WB in WB-W_2B_5 Eutectic Matrix and Pores (Black)

at temperatures in the vicinity of 2020°C was ascertained by metallographic and X-ray inspection of alloys quenched from temperatures varying

Figure 63. W-B (65 At% B), Quenched from 2340°C. X1000
Primary W_2B_5 in a WB-W_2B_5 Eutectic Matrix.

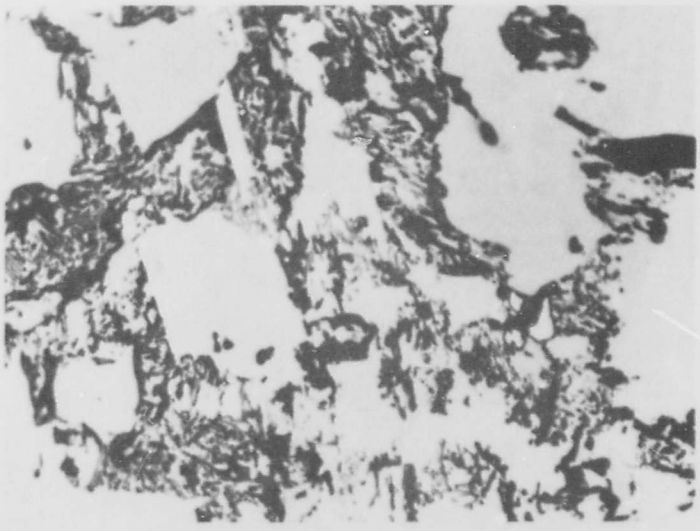

Figure 64. W-B (66 At% B), Quenched from 2340°C. X700
Primary W_2B_5, and WB-W_2B Eutectic

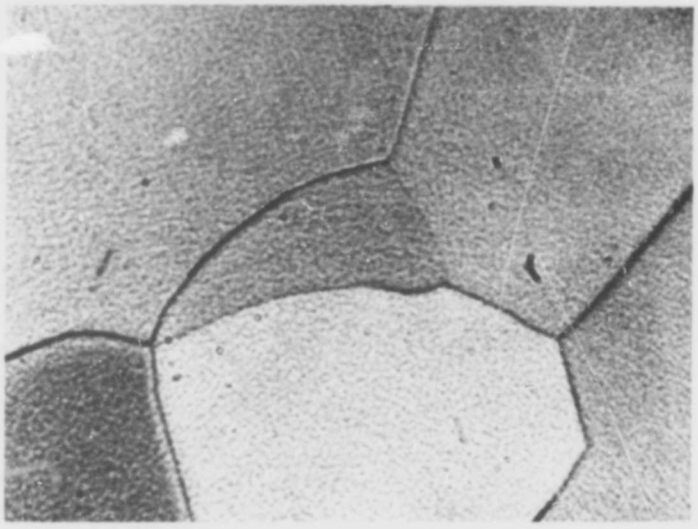

Figure 65. W-B (68 At% B), Rapidly Cooled from 2370°C. X2500
Single Phase W_2B_5
(Vertical Illumination to Reveal Grain Boundaries)

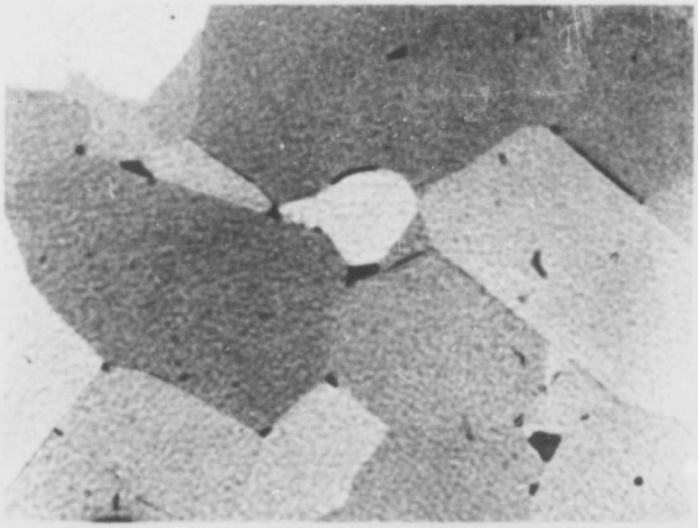

Figure 66. W-B (70 At% B), Melted at 2365°C, Equilibrated X1000
for 2 Minutes at 2100°C, and Quenched.
W_2B_5 with Scant Traces Second Phase at the Grain Boundaries

between 1950 and 2100°C. The X-ray results are supported by a plot of measured incipient melting-temperatures (Figure 41) which indicate a slight decrease of the melting temperatures at boron concentration above 90 At%. The microstructure of an alloy with a nominal boron concentration

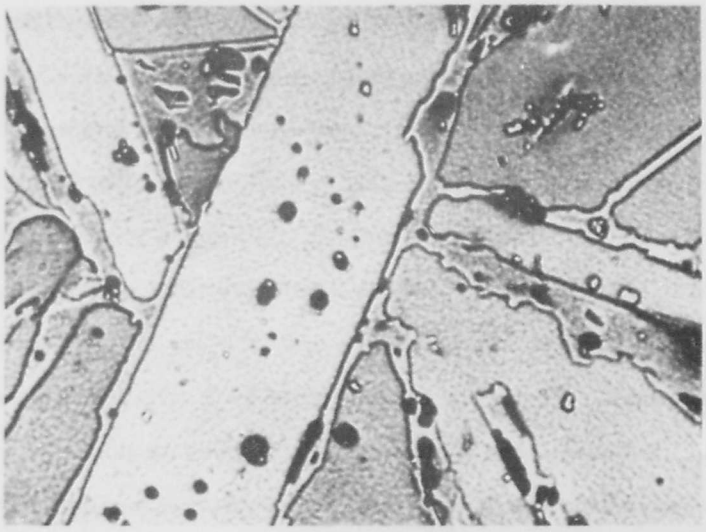

Figure 67. W-B (86 At% B), Melted at 2180°C and Reannealed for 1 hr at 1800°C X1000
$WB_{\sim 12}$ with W_2B_5 at the Grain Boundaries

of 86 At% shows $WB_{\sim 12}$ and smaller amounts of W_2B_5 (Figure 67). The metal-rich boundary of the high-boron phase in this system is therefore located at still higher boron concentration.

The experimental findings have been combined in the phase diagram of the system tungsten-boron, which is shown in Figure 2.

IV. DISCUSSION

The phase diagram of the system molybdenum-boron derived from the present investigations, follows in its basic layout the diagram proposed by R. Steinitz and co-workers[3], although significantly higher temperatures (200 - 400°C) were found for the reaction isotherms and the melting temperatures of the intermediate phases. This result is not surprising, since the melting point measurements in the work by R. Steinitz, et.al. were carried out in graphite containers under hydrogen; hence, one would suspect that their melting point data actually refer to eutectic equilibria of the ternary system Mo-B-C; the same arguments also apply to the work by P. W. Gilles and B. D. Pollock[4], which used a similar technique.

The picture regarding the existence of Mo_3B_2 as a high temperature phase is not quite clear. From the experiments by R. Steinitz, et.al.[3] there seems to be no doubt, that a phase was observed in this concentration range. On the other hand, the low melting temperatures reported would indicate a heavy carbon pickup in their melting experiments. According to the well-established ternary Mo-B-C diagram[9], as first caburization product of Mo_2B or Mo_2B + MoB - containing alloys, Mo_2C would appear. Further carbon additions result in the formation of a ternary compound Mo_2BC. This leads one to suspect that it was actually that phase, which was observed in Steinitz's experiments, and referred to as Mo_3B_2.

The data given by Gilles and Pollock in a subsequent work are too sketchy and incomplete, to allow any further conclusions to be drawn with regard to the existence or nature of this compound.

A Wittman, et.al.[10], investigating the ternary alloy system Ti-Mo-B, observed a U_3Si_2-type compound and attributed the occurrence of this phase

to titanium-stabilization of the high temperature phase Mo_3B_2 to lower temperatures. It is uncertain, whether their lattice parameter data given for Mo_3B_2 refer to a ternary solid solution with titanium, or whether they were measured on the pure binary compound.

In our investigations, the occurrence of a compound Mo_3B_2 was not observed in any of the experiments performed to contest the previous findings. Since higher purity materials and more refined investigation techniques were used in this investigation, we conclude, that the existence of Mo_3B_2 as a pure binary compound is highly unlikely.

In the tungsten-boron system, all the previously known phases were confirmed. The phase diagram established in the present work basically follows the estimated diagram by R. Kieffer and F. Benesovsky[1] (Figure 5), although somewhat different values were found for the homogeneity ranges and the melting temperatures of the intermediate phases and the eutectic reaction isotherms.

An interesting finding in both systems concerns the morphology of the metal-rich eutectics. Analogous structures have meanwhile been found in other binary and ternary metal-carbon systems. Systematic studies of the factors governing the morphology of eutectic and eutectoid structures could lead to the development of composite structures with interesting properties.

REFERENCES

(1) Compare R. Kieffer and F. Benesovsky: Hartstoffe (Wien, Springer, 1963).

(2) R. Kiessling: Acta Chem. Scand. 1 (1947), 893.

(3) R. Steinitz, L. Binder, and D. Moskowitz: J. Metals 4 (1952), 983.

(4) P.W. Gilles and B.D. Pollock: J. Metals 5 (1953), 1537.

(5) L. Andrieux and G. Weiss: Bull.Soc. Chim.France 15 (1948), 598.

(6) R. Kiessling: Acta. Chem. Scand. 4 (1950), 209.

(7) F. Bertaut and P. Blum: Acta. Cryst. 4 (1951), 72.

(8) A. Chretien and J. Helgorsky: Compt.Rend. 225 (1961), 742.

(9) E. Rudy, F. Benesovsky, and L.E. Toth: Z. Metallkde, 54, (1963), 345.

(10) A. Wittmann, H. Nowotny, and H. Boller: Mh. Chem. 91 (1960), 608.

(11) Climax Molybdenum Company, Second Annual Report, 1951 (Work Quoted in M. Hansen, Constitution of Binary Alloys, McGraw-Hill, New York, 1958).

(12) R. Kieffer, F. Benesovsky, and E. R. Honak: Z. anorg. Chemie, 268 (1952), 191.

(13) B. Post and F. W. Glaser: J. Chem. Phys. 20 (1952), 1050.

(14) G. V. Samsonov: Dokl. Acad.Nauk SSSR 113 (1957), 1299.

(15) F. W. Glaser: J. Metals, 4 (1952), 391.

(16) L. Brewer, D.L. Sawyer, D.H. Templeton, and C.H. Dauben: J. Am. Ceram. Soc. 34 (1951), 173.

(17) E.R. Honak: Diss.Techn. Hochschule Graz, 1951.

(18) C. Agte: Diss. Techn. Hochschule Berlin, 1931

(19) P. Schwarzkopf and F.Glaser: Z.Metallkde 44 (1953), 353

(20) E. Rudy, St. Windisch, and Y.A. Chang: AFML-TR-65-2, Part I, Vol.I (January 1965).

DOCUMENT CONTROL DATA - R&D

(Security classification of title, body of abstract and indexing annotation must be entered when the overall report is classified)

1. ORIGINATING ACTIVITY *(Corporate author)*
(5) Materials Research Laboratory
Aerojet-General Corporation
Sacramento, California (upper case)

2a. REPORT SECURITY CLASSIFICATION
Unclassified

2b. GROUP
N.A.

3. REPORT TITLE
(6) Ternary Phase Equilibria in Transition Metal-Boron-Carbon-Silicon Systems.

Part I. Related Binary Systems, Volume III. Systems Mo-B and W-B

4. DESCRIPTIVE NOTES *(Type of report and inclusive dates)*
(9) Technical Documentary Report, 1 November 1964 to 1 June 1965,

5. AUTHOR(S) *(Last name, first name, initial)*
(10) by
Rudy, Erwin Rudy and
Windisch, Stefan Windisch.

6. REPORT DATE
(11) May 1965,

7a. TOTAL NO. OF PAGES
(12) 72 p.

7b. NO. OF REFS
20

8a. CONTRACT OR GRANT NO.
(15) AF 33(615)-1249,

8b. PROJECT NO.
(16) AF 7350,

8c. Task No. 735001
(17)

8d.

9a. ORIGINATOR'S REPORT NUMBER(S)
(18) AFML-TR-65-2-Pt-I-Vol-3
Part I, Vol. III

9b. OTHER REPORT NO(S) *(Any other numbers that may be assigned this report)*
N.A.

10. AVAILABILITY/LIMITATION NOTICES
Qualified requesters may obtain copies of this report from DDC

11. SUPPLEMENTARY NOTES

12. SPONSORING MILITARY ACTIVITY
AFML (MAMC)
Wright-Patterson Air Force Base, Ohio 45433

13. ABSTRACT

On the basis of X-ray, melting point, metallographic, and differential thermoanalytical studies on molybdenum-boron and tungsten-boron alloys, constitution diagrams for both binary systems are presented. In the high temperature regions, the newly established phase diagrams differ significantly from previously reported systems.

The results are discussed and compared with available literature data.

DD FORM 1 JAN 64 1473

UNCLASSIFIED
Security Classification

UNCLASSIFIED

Security Classification

14. KEY WORDS	LINK A		LINK B		LINK C	
	ROLE	WT	ROLE	WT	ROLE	WT
Boride Binary Systems Phase Equilibria						

INSTRUCTIONS

1. ORIGINATING ACTIVITY: Enter the name and address of the contractor, subcontractor, grantee, Department of Defense activity or other organization *(corporate author)* issuing the report.

2a. REPORT SECURITY CLASSIFICATION: Enter the overall security classification of the report. Indicate whether "Restricted Data" is included. Marking is to be in accordance with appropriate security regulations.

2b. GROUP: Automatic downgrading is specified in DoD Directive 5200.10 and Armed Forces Industrial Manual. Enter the group number. Also, when applicable, show that optional markings have been used for Group 3 and Group 4 as authorized.

3. REPORT TITLE: Enter the complete report title in all capital letters. Titles in all cases should be unclassified. If a meaningful title cannot be selected without classification, show title classification in all capitals in parenthesis immediately following the title.

4. DESCRIPTIVE NOTES: If appropriate, enter the type of report, e.g., interim, progress, summary, annual, or final. Give the inclusive dates when a specific reporting period is covered.

5. AUTHOR(S): Enter the name(s) of author(s) as shown on or in the report. Enter last name, first name, middle initial. If military, show rank and branch of service. The name of the principal author is an absolute minimum requirement.

6. REPORT DATE: Enter the date of the report as day, month, year; or month, year. If more than one date appears on the report, use date of publication.

7a. TOTAL NUMBER OF PAGES: The total page count should follow normal pagination procedures, i.e., enter the number of pages containing information.

7b. NUMBER OF REFERENCES: Enter the total number of references cited in the report.

8a. CONTRACT OR GRANT NUMBER: If appropriate, enter the applicable number of the contract or grant under which the report was written.

8b, 8c, & 8d. PROJECT NUMBER: Enter the appropriate military department identification, such as project number, subproject number, system numbers, task number, etc.

9a. ORIGINATOR'S REPORT NUMBER(S): Enter the official report number by which the document will be identified and controlled by the originating activity. This number must be unique to this report.

9b. OTHER REPORT NUMBER(S): If the report has been assigned any other report numbers *(either by the originator or by the sponsor)*, also enter this number(s).

10. AVAILABILITY/LIMITATION NOTICES: Enter any limitations on further dissemination of the report, other than those imposed by security classification, using standard statements such as:

(1) "Qualified requesters may obtain copies of this report from DDC."

(2) "Foreign announcement and dissemination of this report by DDC is not authorized."

(3) "U. S. Government agencies may obtain copies of this report directly from DDC. Other qualified DDC users shall request through

_____."

(4) "U. S. military agencies may obtain copies of this report directly from DDC. Other qualified users shall request through

_____."

(5) "All distribution of this report is controlled. Qualified DDC users shall request through

_____."

If the report has been furnished to the Office of Technical Services, Department of Commerce, for sale to the public, indicate this fact and enter the price, if known.

11. SUPPLEMENTARY NOTES: Use for additional explanatory notes.

12. SPONSORING MILITARY ACTIVITY: Enter the name of the departmental project office or laboratory sponsoring *(paying for)* the research and development. Include address.

13. ABSTRACT: Enter an abstract giving a brief and factual summary of the document indicative of the report, even though it may also appear elsewhere in the body of the technical report. If additional space is required, a continuation sheet shall be attached.

It is highly desirable that the abstract of classified reports be unclassified. Each paragraph of the abstract shall end with an indication of the military security classification of the information in the paragraph, represented as *(TS), (S), (C), or (U)*.

There is no limitation on the length of the abstract. However, the suggested length is from 150 to 225 words.

14. KEY WORDS: Key words are technically meaningful terms or short phrases that characterize a report and may be used as index entries for cataloging the report. Key words must be selected so that no security classification is required. Identifiers, such as equipment model designation, trade name, military project code name, geographic location, may be used as key words but will be followed by an indication of technical context. The assignment of links, roles, and weights is optional.

UNCLASSIFIED

Security Classification